Electronic Supplementary Material (ESI) for Catalysis Science & Technology.

Supporting Information
for

Salt-Promoted Catalytic Methanol Carbonylation Using Iridium Pincer-Crown Ether Complexes

*Lauren C. Gregor,[‡] Javier Grajeda,[‡] Peter S. White,[‡] Andrew J. Vetter,[§] and Alexander J. M. Miller[‡]**

[‡] *Department of Chemistry, University of North Carolina at Chapel Hill, Chapel Hill, North Carolina 27599-3290, United States*

[§] *Eastman Chemical Company, Kingsport, Tennessee 37660, United States*

ajmm@email.unc.edu

Table of Contents

I. NMR Spectra of New Compounds

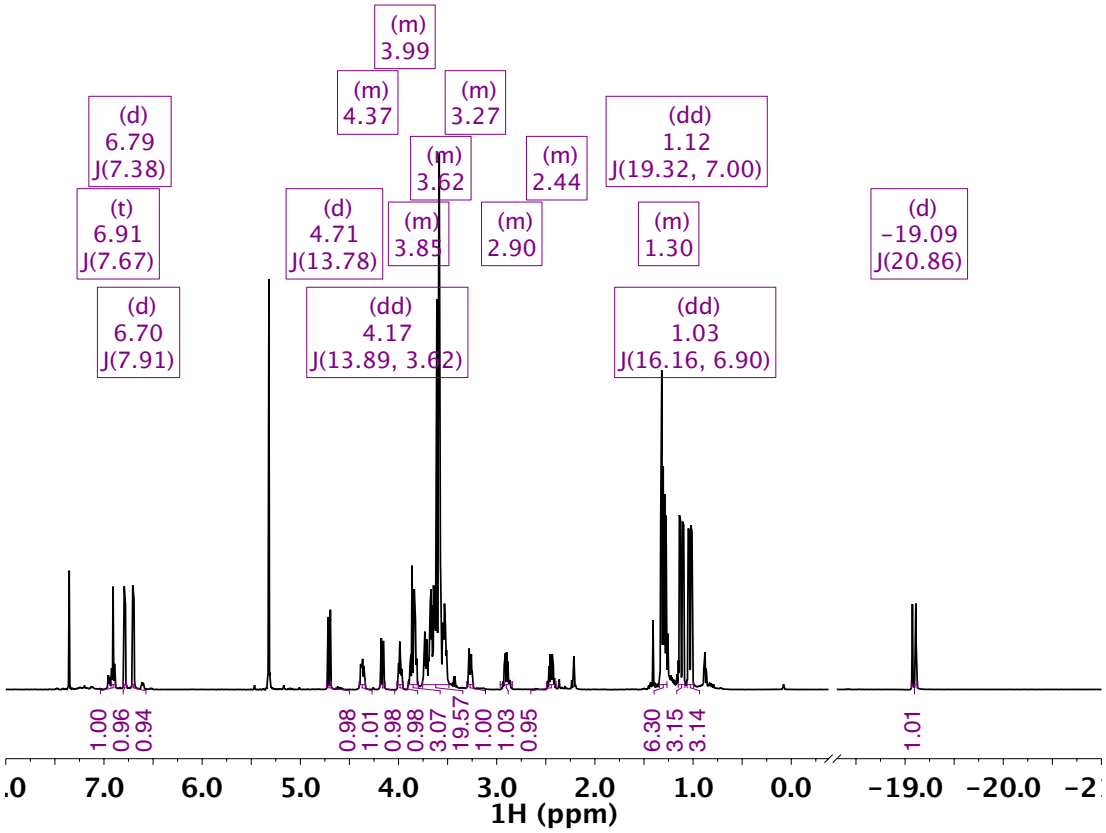

Figure S1. ^{1}H NMR spectrum of κ^3-(^{18c6}NCOP^{iPr})Ir(H)(CO)(Cl) (**1**$^{\mathbf{18c6}}$) in CD_2Cl_2.

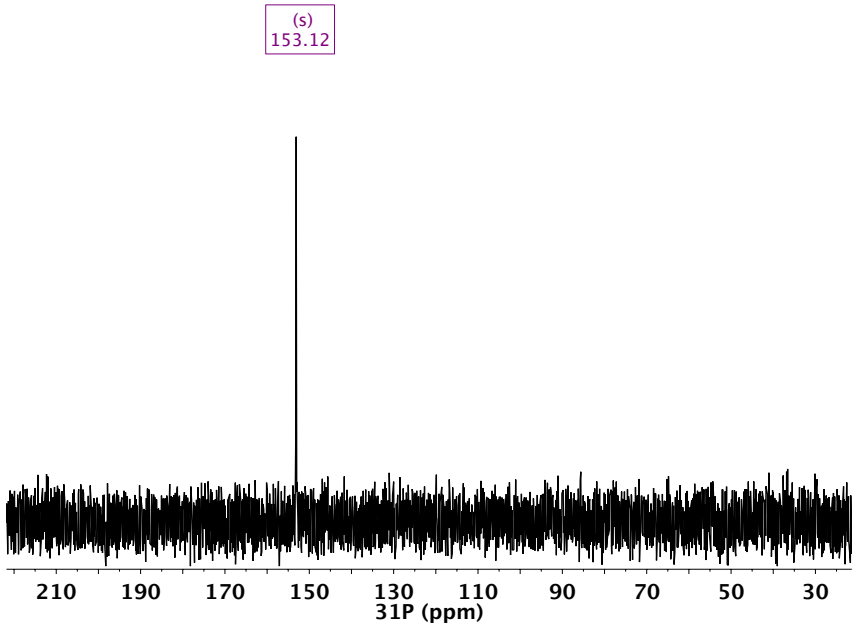

Figure S2. ^{31}P{^{1}H} NMR spectrum of κ^3-(^{18c6}NCOP^{iPr})Ir(H)(CO)(Cl) (**1**$^{\mathbf{18c6}}$) in CD_2Cl_2.

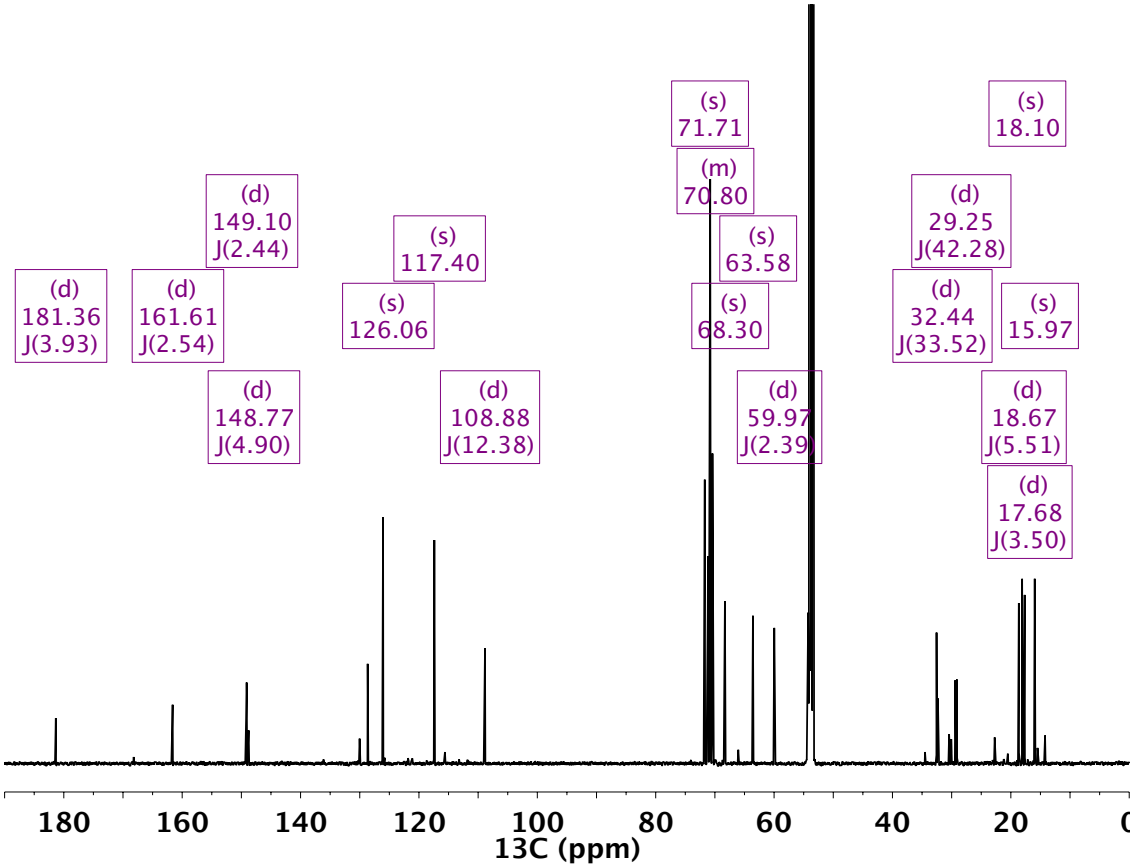

Figure S3. $^{13}C\{^{1}H\}$ NMR spectrum of κ^3-(^{18c6}NCOP^{iPr})Ir(H)(CO)(Cl) (**1**$^{\mathbf{18c6}}$) in CD_2Cl_2.

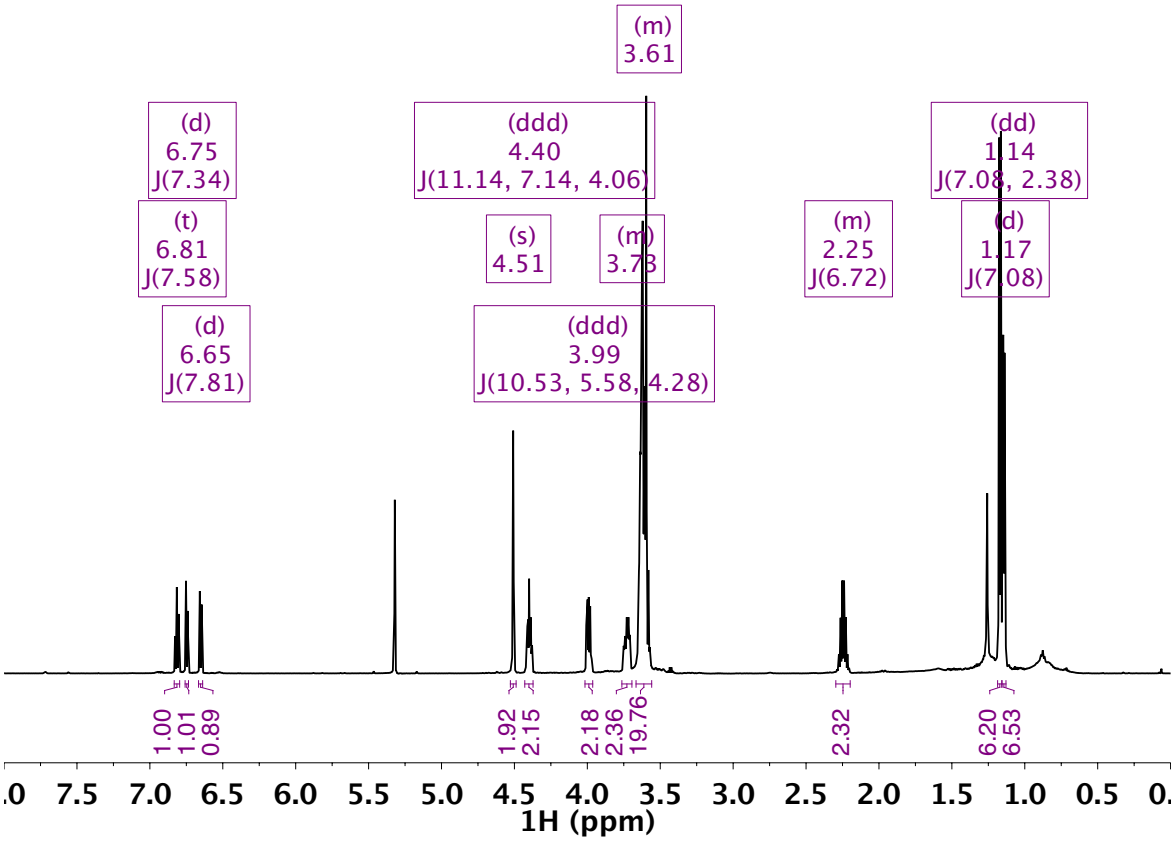

Figure S4. ^{1}H NMR spectrum of κ^3-(^{18c6}NCOP^{iPr})Ir(CO) (**2**$^{\mathbf{18c6}}$) in CD_2Cl_2.

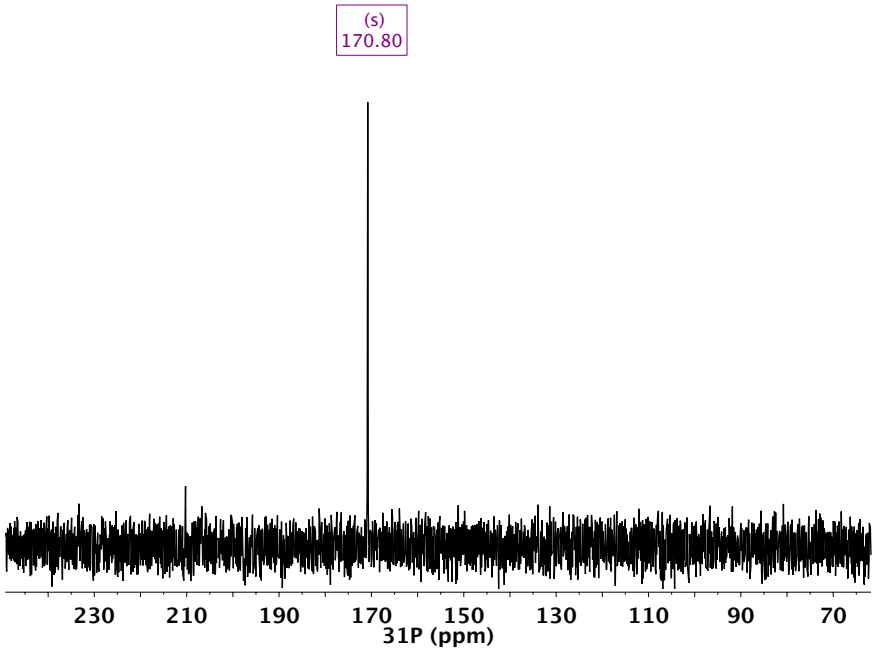

Figure S5. ^{31}P{^{1}H} NMR spectrum of κ^3-(^{18c6}NCOP^{iPr})Ir(CO) (**2**$^{\mathbf{18c6}}$) in CD_2Cl_2.

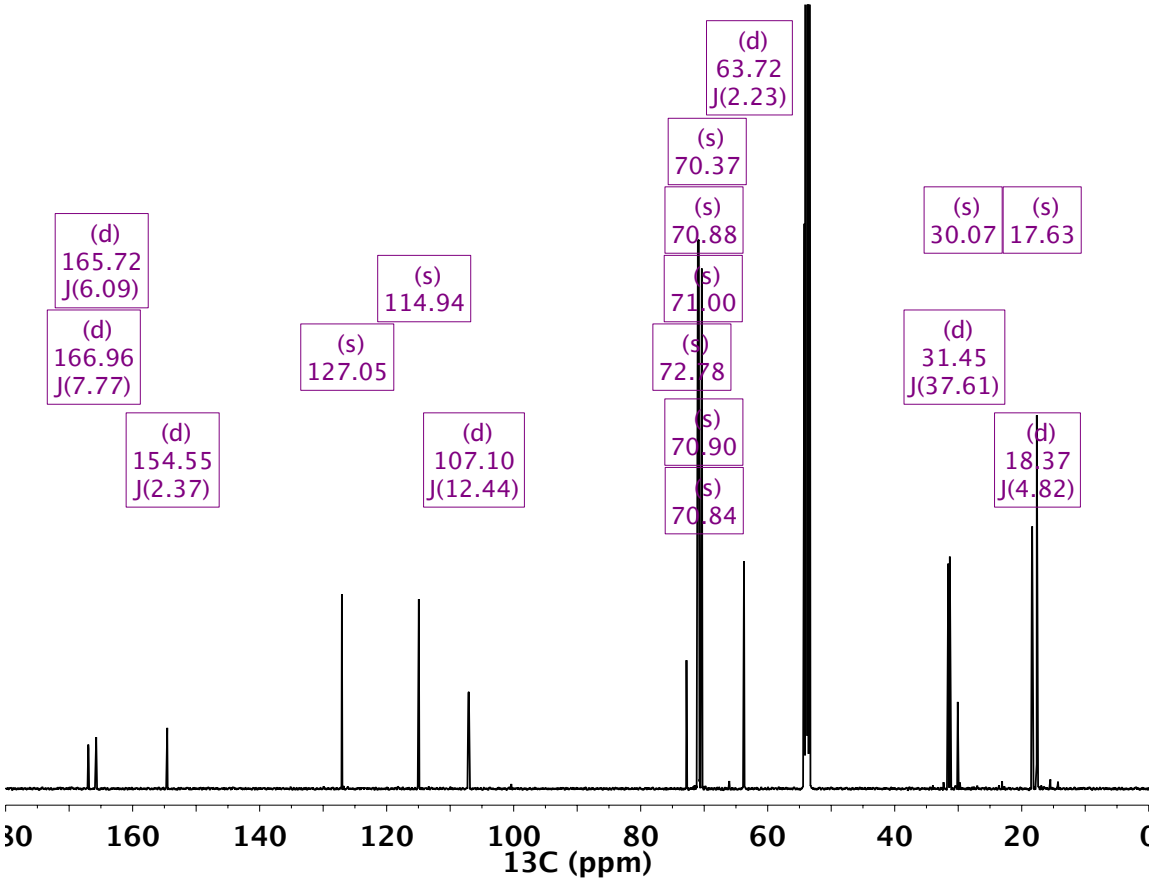

Figure S6. $^{13}C\{^{1}H\}$ NMR spectrum of κ^3-(^{18c6}NCOP^{iPr})Ir(CO) (**2**$^{\mathbf{18c6}}$) in CD_2Cl_2.

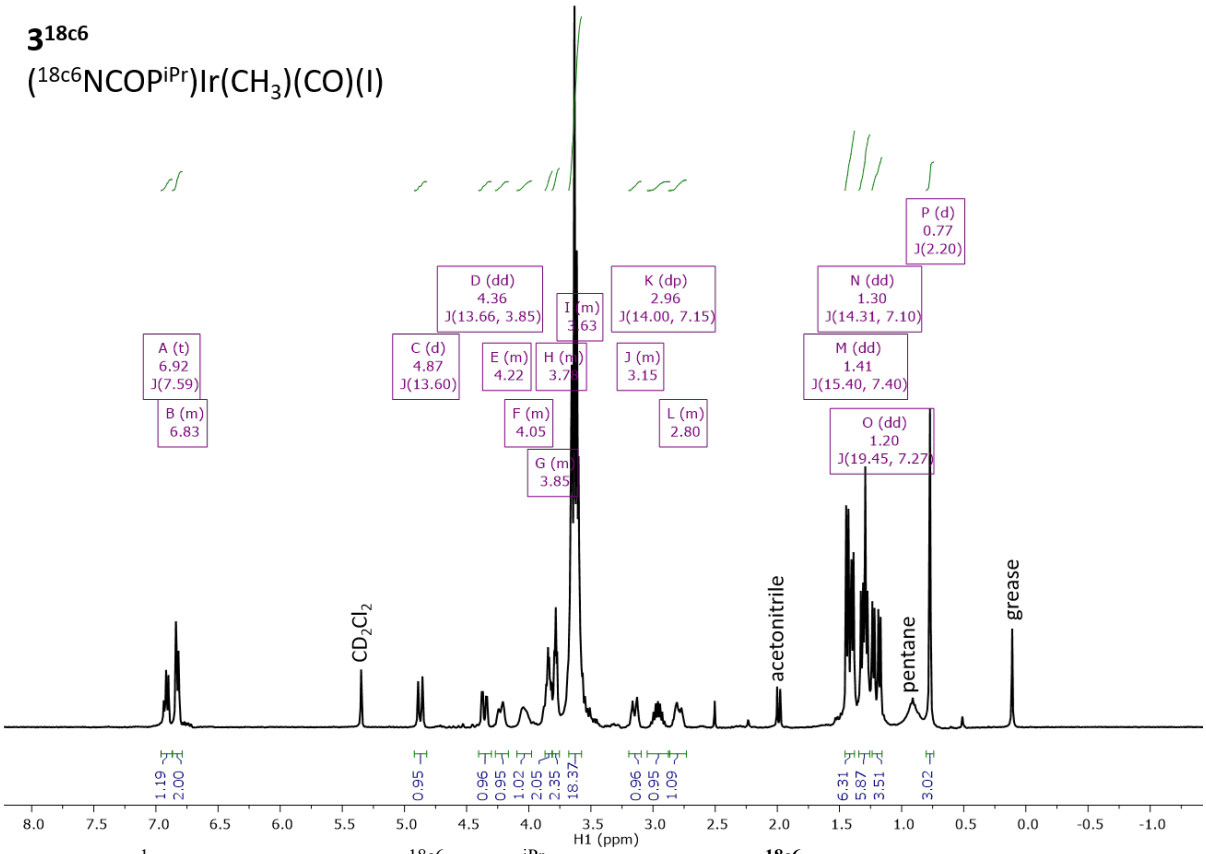

Figure S7. ^{1}H NMR spectrum of (^{18c6}NCOP^{iPr})Ir(CH$_3$)(CO)(I) (**3^{18c6}**) in CD_2Cl_2.

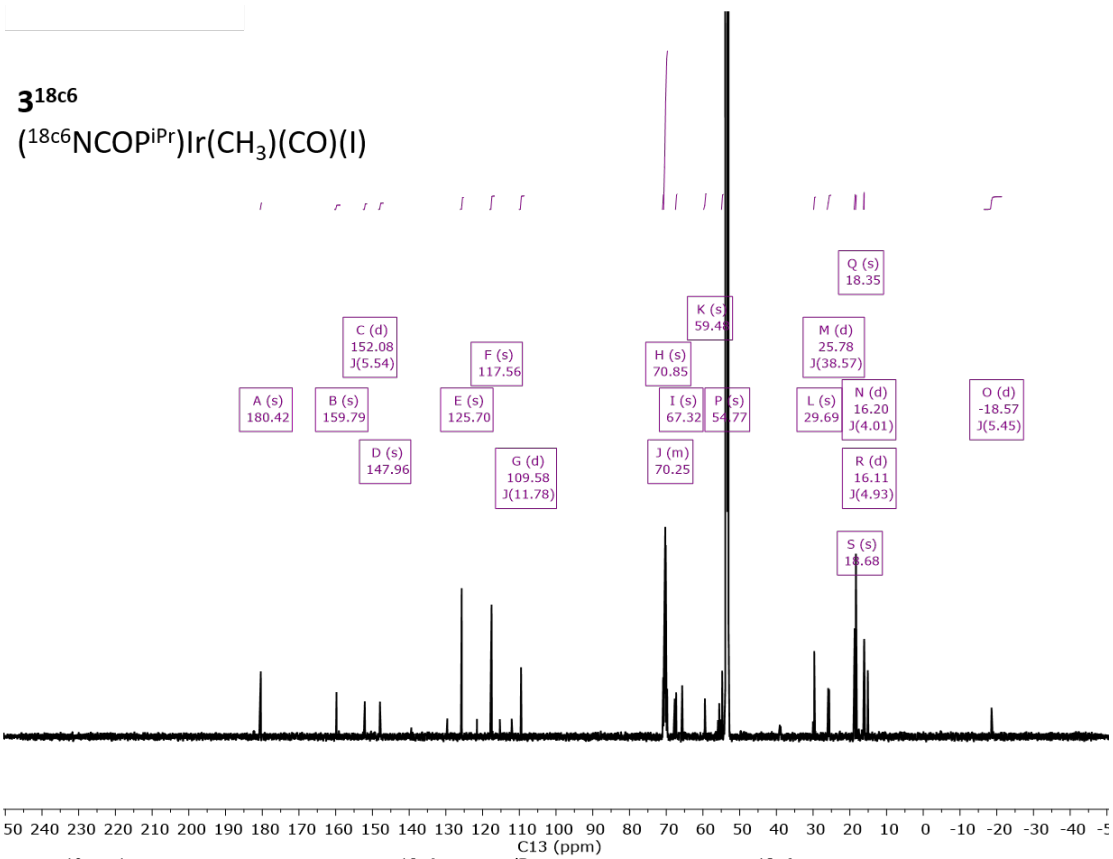

Figure S8. $^{13}C\{^{1}H\}$ NMR spectrum of ($^{18c6}NCOP^{iPr}$)Ir(CH_3)(CO)(I) (**3**^{18c6}) in CD_2Cl_2.

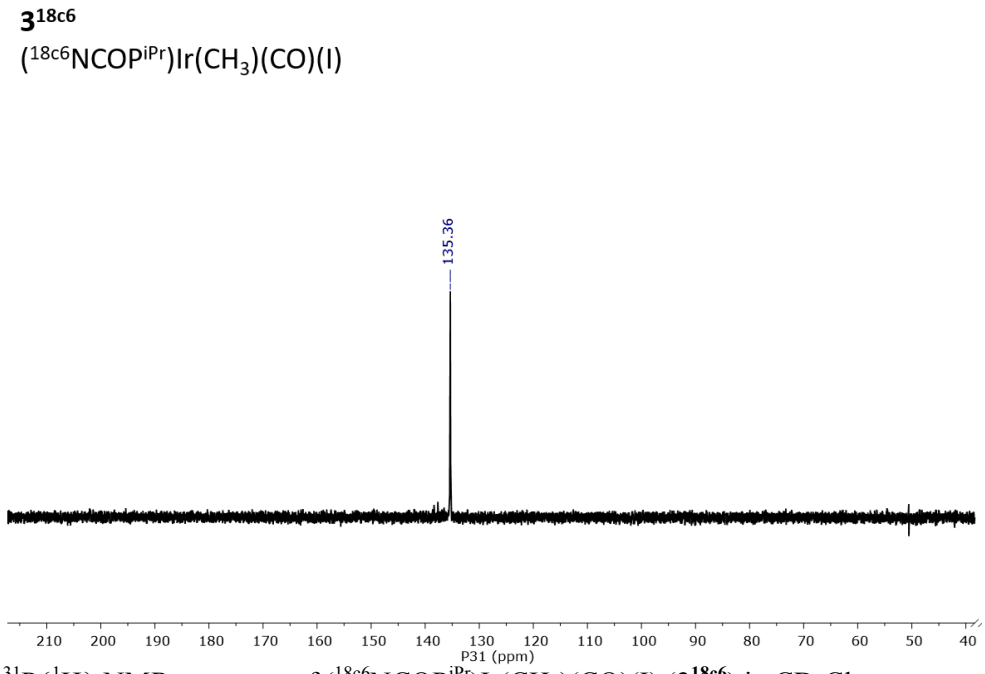

Figure S9. $^{31}P\{^{1}H\}$ NMR spectrum of ($^{18c6}NCOP^{iPr}$)Ir(CH_3)(CO)(I) (**3**^{18c6}) in CD_2Cl_2.

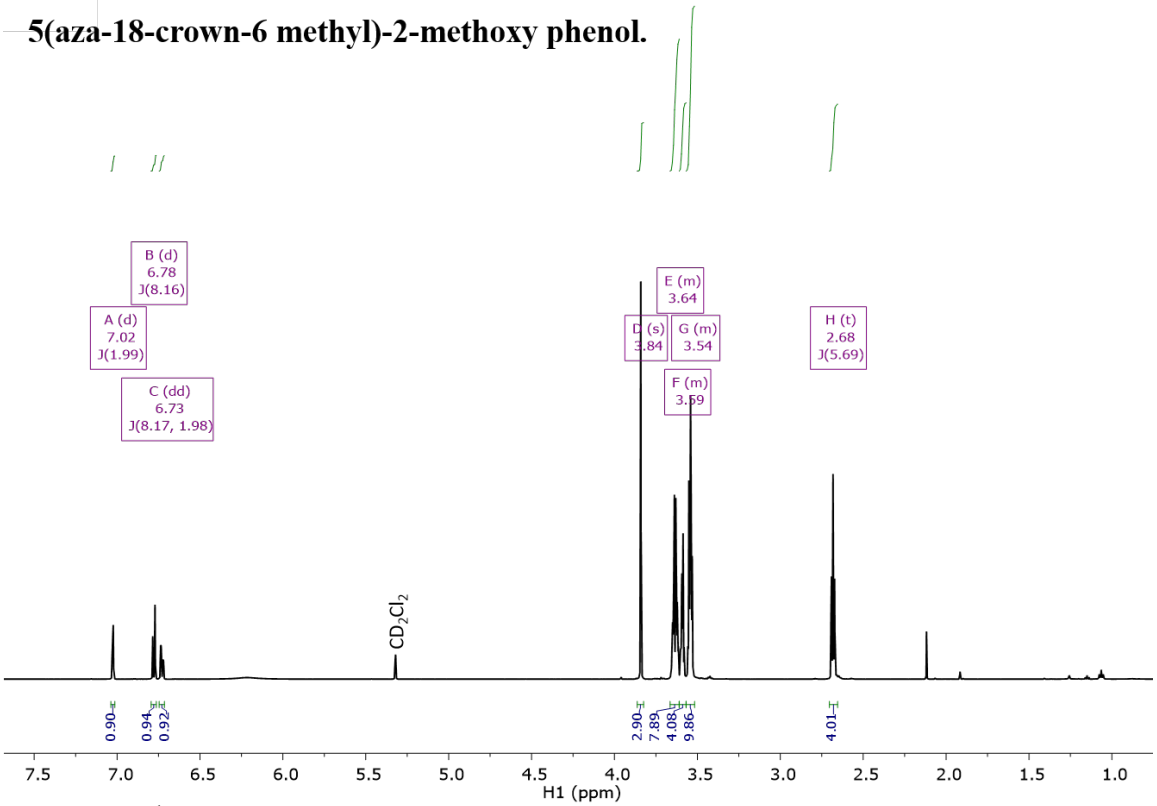

Figure S10. ^{1}H NMR spectrum of 5-(aza-18-crown-6 methyl)-2-methoxy phenol in CD_2Cl_2.

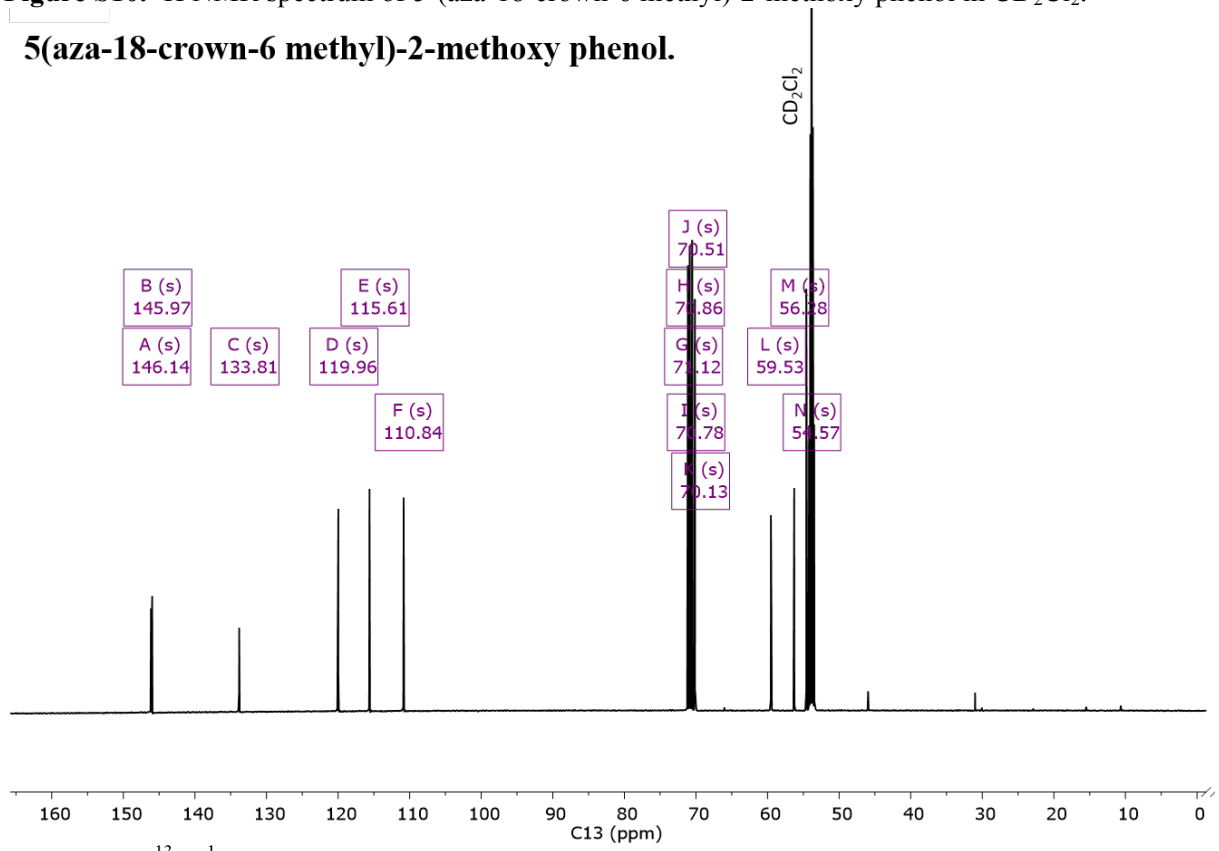

Figure S11. $^{13}C\{^{1}H\}$ NMR spectrum of 5-(aza-18-crown-6 methyl)-2-methoxy phenol in CD_2Cl_2.

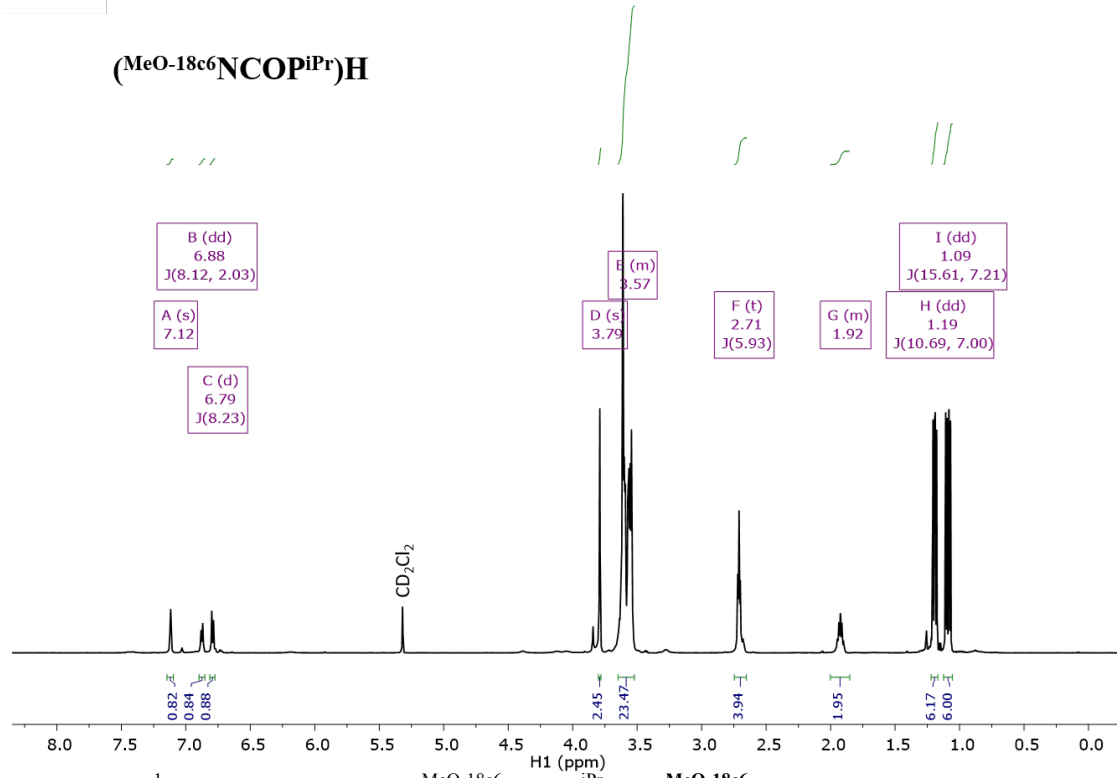

Figure S12. ^{1}H NMR spectrum of ($^{MeO\text{-}18c6}$NCOP^{iPr})H (**5**$^{\mathbf{MeO\text{-}18c6}}$) ligand in CD_2Cl_2.

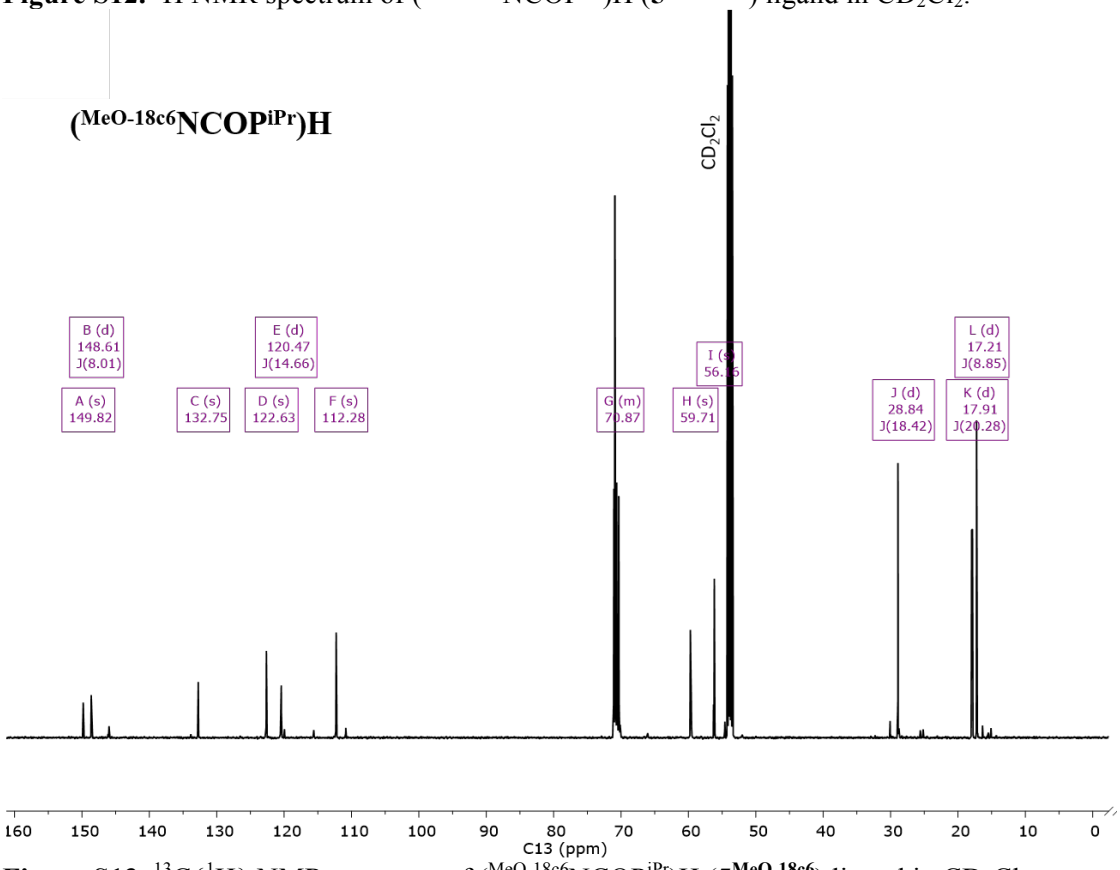

Figure S13. ^{13}C{^{1}H} NMR spectrum of ($^{MeO\text{-}18c6}$NCOP^{iPr})H (**5**$^{\mathbf{MeO\text{-}18c6}}$) ligand in CD_2Cl_2.

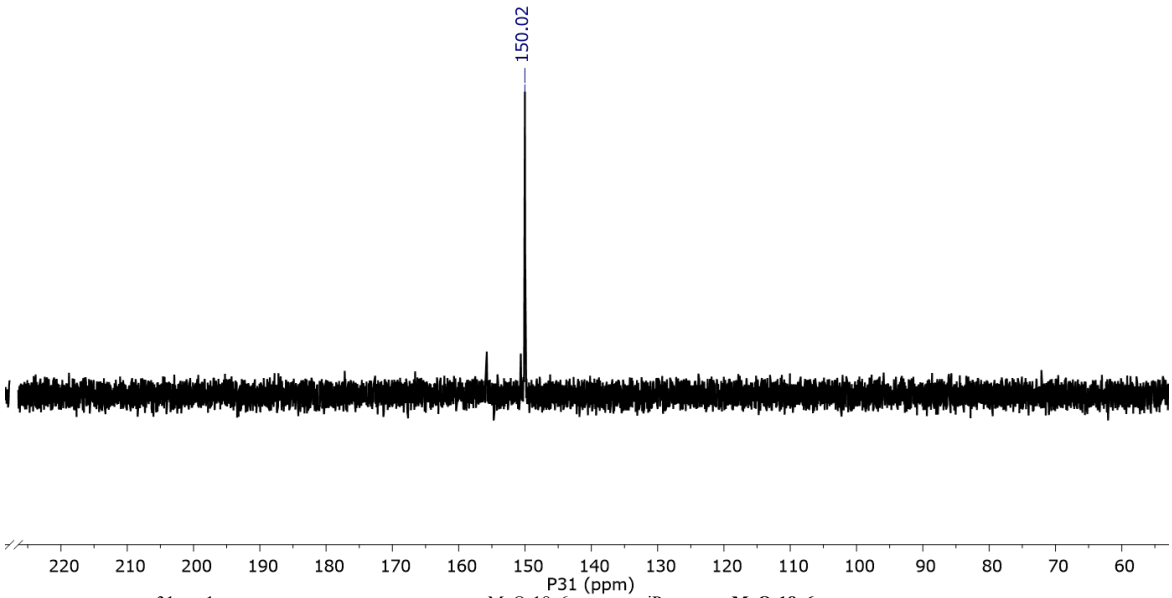

Figure S14. $^{31}P\{^{1}H\}$ NMR spectrum of ($^{MeO\text{-}18c6}$NCOP^{iPr})H (**5**$^{MeO\text{-}18c6}$) ligand in CD_2Cl_2.

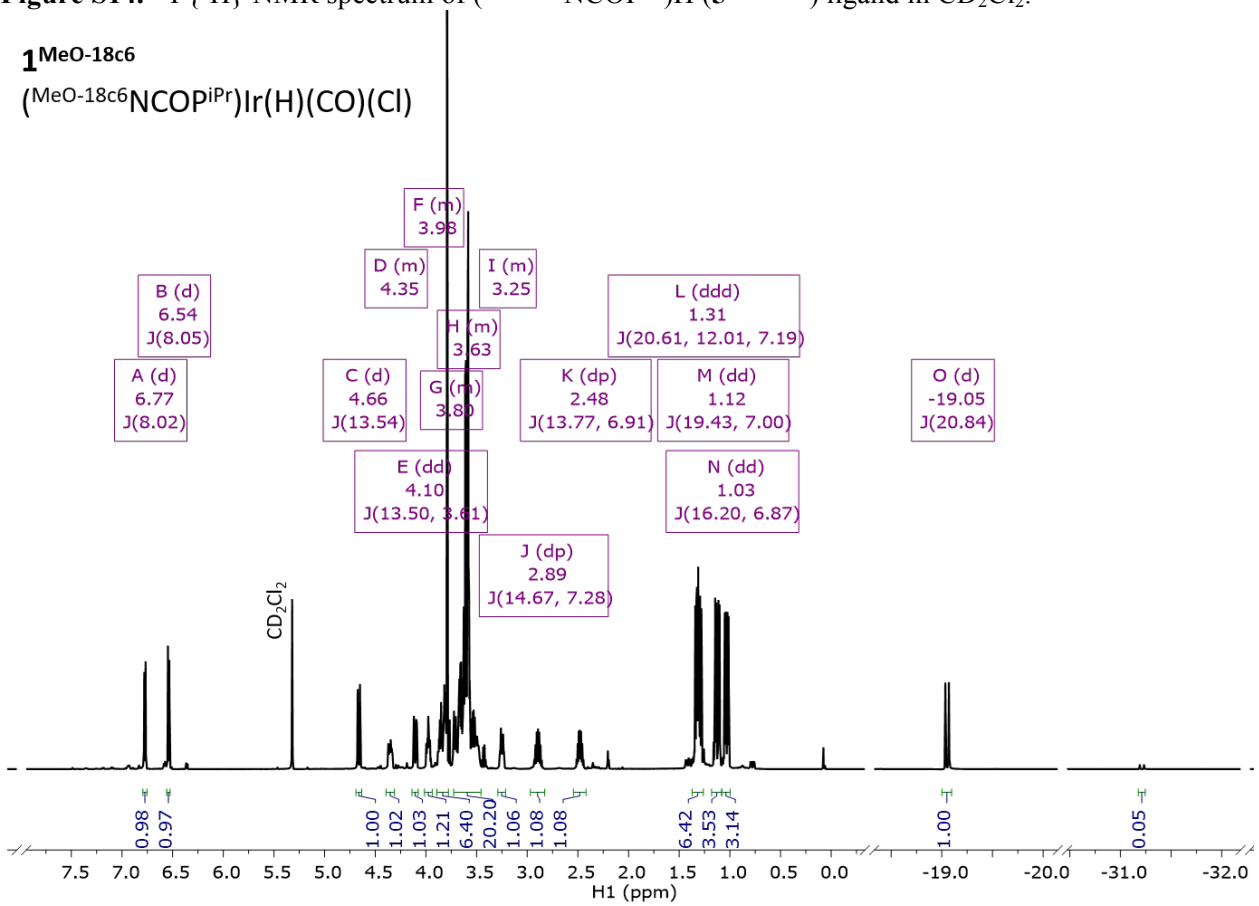

Figure S15. ^{1}H NMR spectrum of ($^{MeO\text{-}18c6}$NCOP^{iPr})Ir(H)(CO)(Cl) (**1**$^{MeO\text{-}18c6}$) in CD_2Cl_2. A second Ir-H is present (δ -31) which integrates to less than 5% relative to the major species.

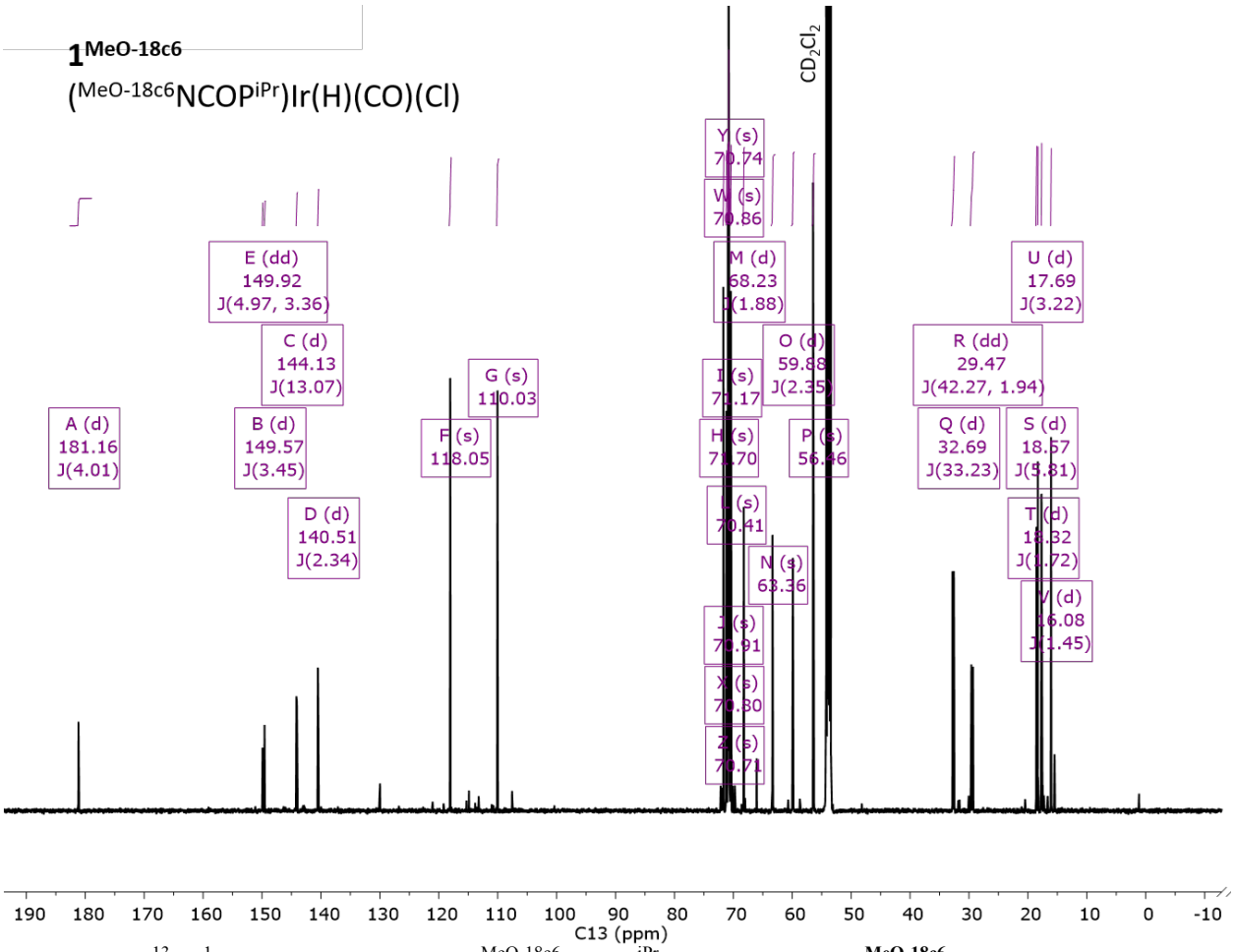

Figure S16. $^{13}C\{^{1}H\}$ NMR spectrum of ($^{MeO\text{-}18c6}NCOP^{iPr}$)Ir(H)(CO)(Cl) (**1**$^{\textbf{MeO-18c6}}$) in CD_2Cl_2.

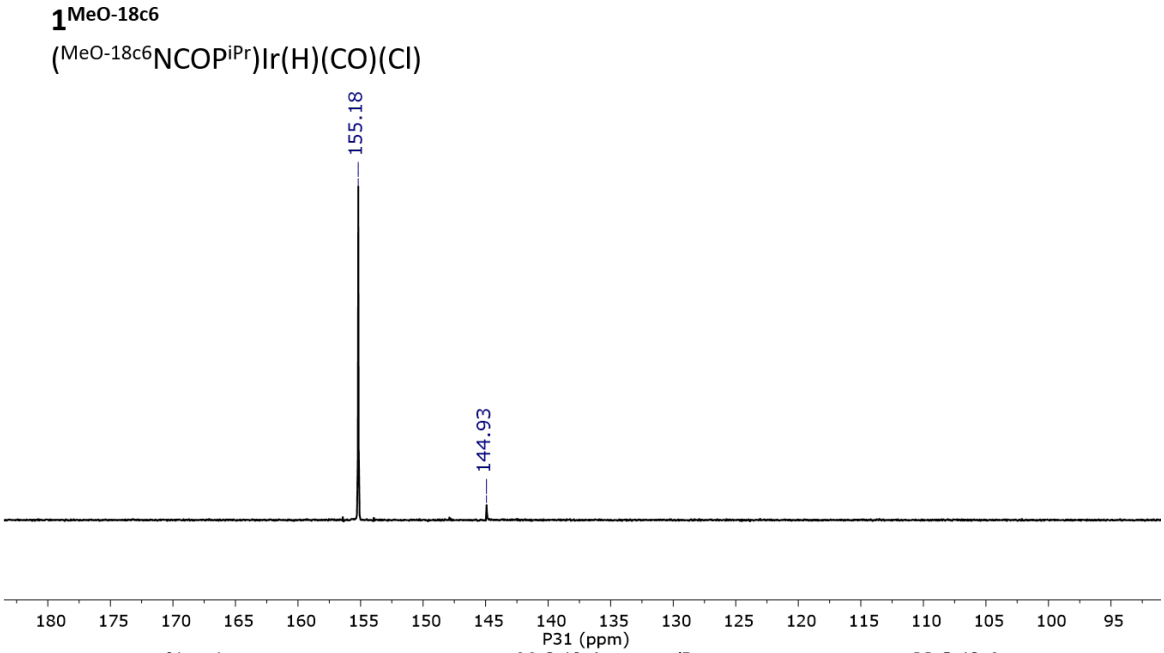

Figure S17. $^{31}P\{^{1}H\}$ NMR spectrum of ($^{MeO\text{-}18c6}NCOP^{iPr}$)Ir(H)(CO)(Cl) (**1**$^{\textbf{MeO-18c6}}$) in CD_2Cl_2. A <5% impurity is observed (δ 145).

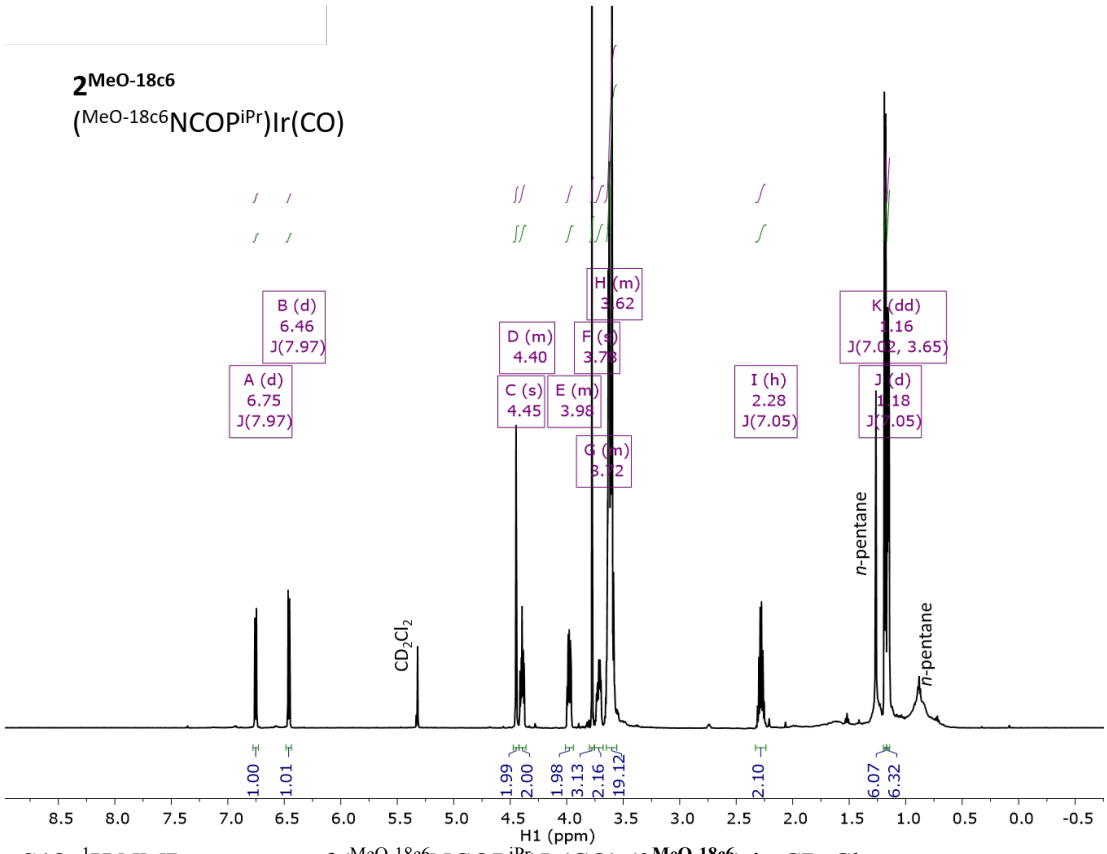

Figure S18. ^{1}H NMR spectrum of ($^{MeO\text{-}18c6}$NCOP^{iPr})Ir(CO) (**2**$^{\mathbf{MeO\text{-}18c6}}$) in CD_2Cl_2.

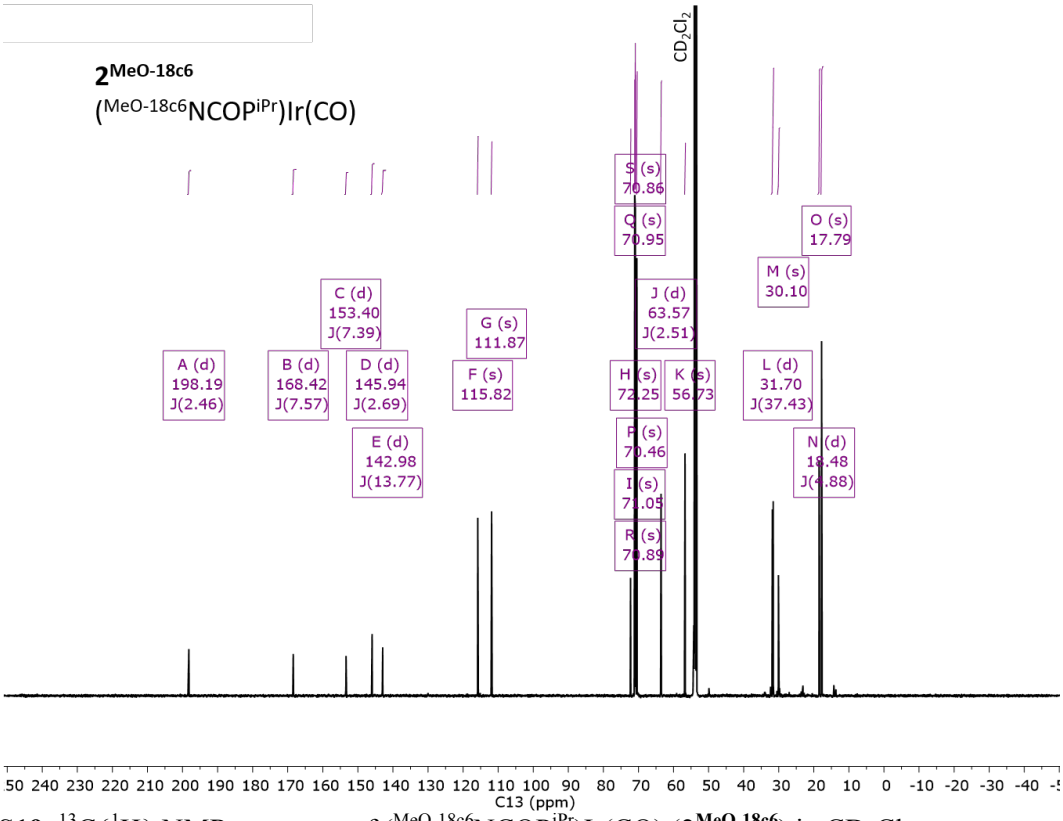

Figure S19. ^{13}C{^{1}H} NMR spectrum of ($^{MeO\text{-}18c6}$NCOP^{iPr})Ir(CO) (**2**$^{\mathbf{MeO\text{-}18c6}}$) in CD_2Cl_2.

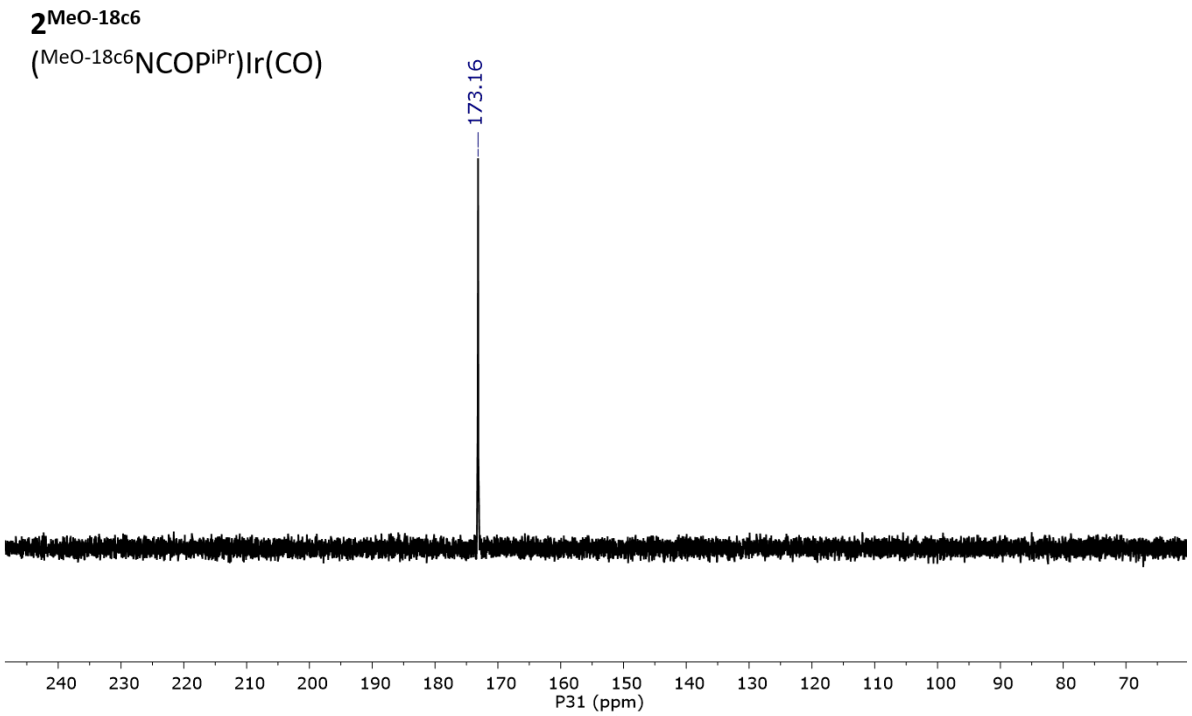

Figure S20. $^{31}P\{^{1}H\}$ spectrum NMR of ($^{MeO\text{-}18c6}NCOP^{iPr}$)Ir(CO) (**2**$^{\mathbf{MeO\text{-}18c6}}$) in CD_2Cl_2.

II. Multireactor Catalysis Data

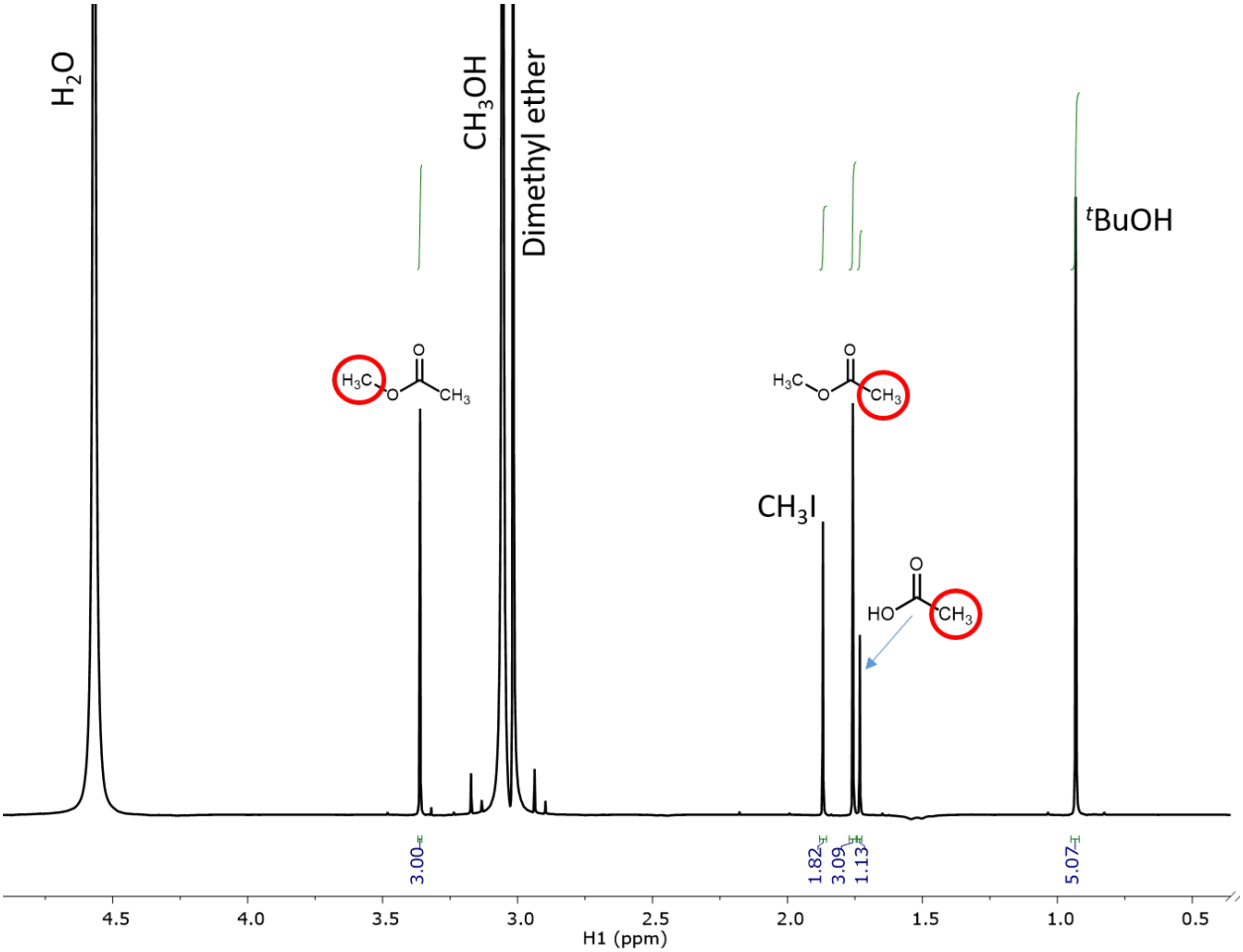

Figure S21. Typical ^{1}H NMR spectrum after multireactor catalysis. Conditions: CH_3OH solution containing ^{t}BuOH internal standard, CD_3OD capillary. The product peaks are set to the representative number of protons (3H for each methyl product synthesized) and relative integration against ^{t}BuOH internal standard is used to calculate the mmol of products:

$$mmol\ products = \frac{mmol\ std.}{\frac{std.\ integration}{9}} = \frac{1.882}{\frac{5.07}{9}} = 3.34\ mmol$$

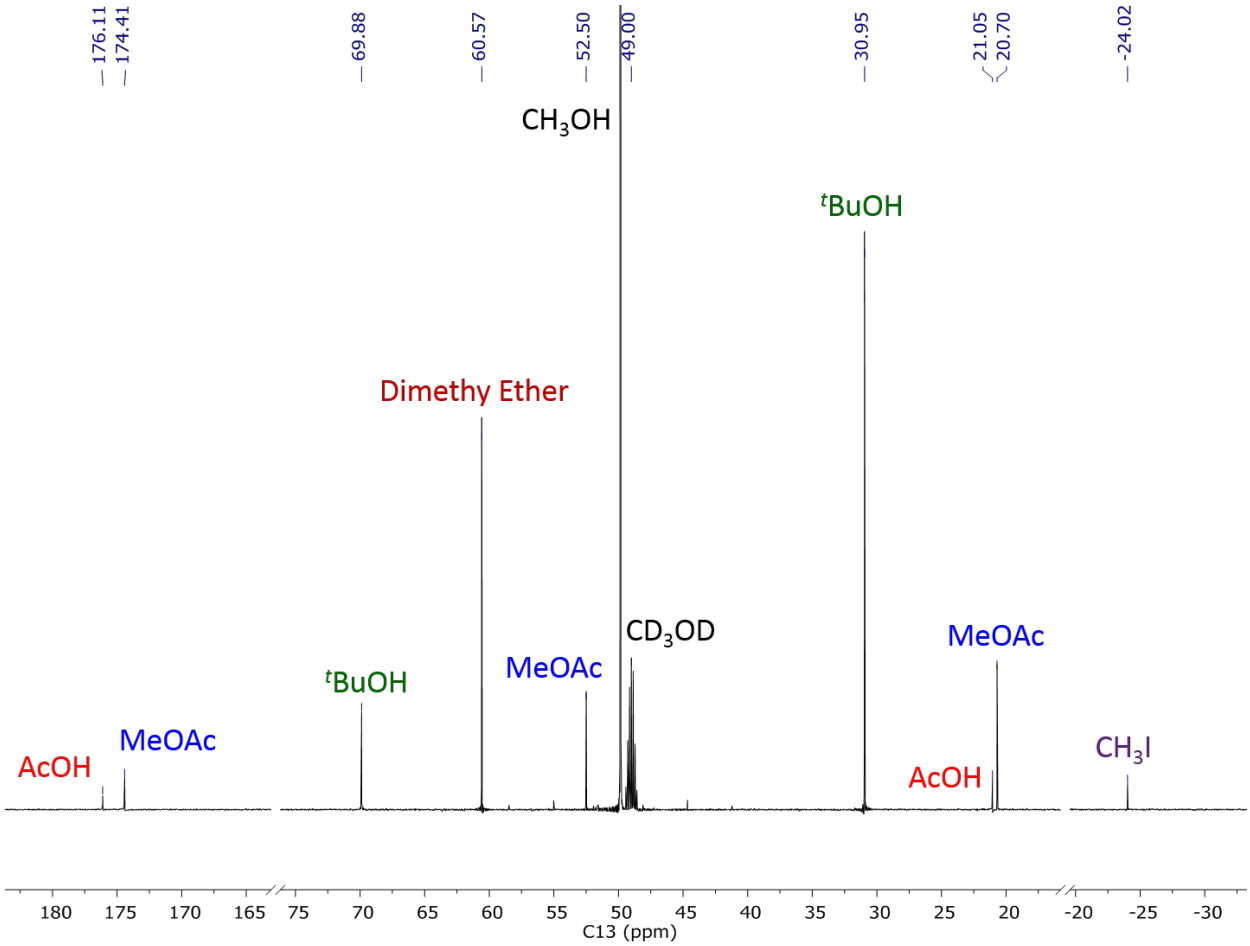

Figure S22. Typical $^{13}C\{^{1}H\}$ NMR spectrum after multireactor catalysis. Conditions: CH_3OH solution containing ^{t}BuOH internal standard, CD_3OD capillary.

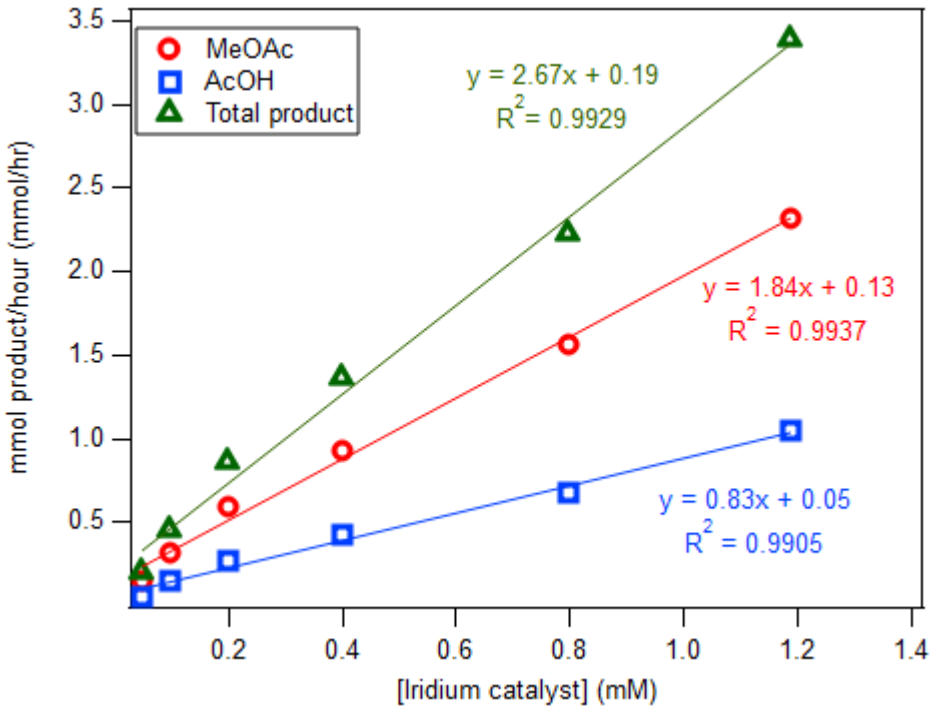

[Ir]	TON MeOAc	TON AcOH	total TON	TOF	mmol MeOAc/hr	mmol AcOH/hr	total acyl/hr
0.05	814	315	1129	376.425	0.14	0.05	0.19
0.1	926	404	1330	443.317	0.31	0.14	0.44
0.2	881	386	1267	422.365	0.59	0.26	0.85
0.4	701	313	1013	337.72	0.93	0.42	1.35
0.8	585	251	836	278.651	1.56	0.67	2.22
1.19	588	266	854	284.666	2.32	1.05	3.38

Figure S23. Iridium dependence of methanol carbonylation reaction with $\mathbf{2}^{\mathbf{18c6}}$. Conditions: 150 °C, 3 hours and 25 bar CO with 0.5 M CH_3I.

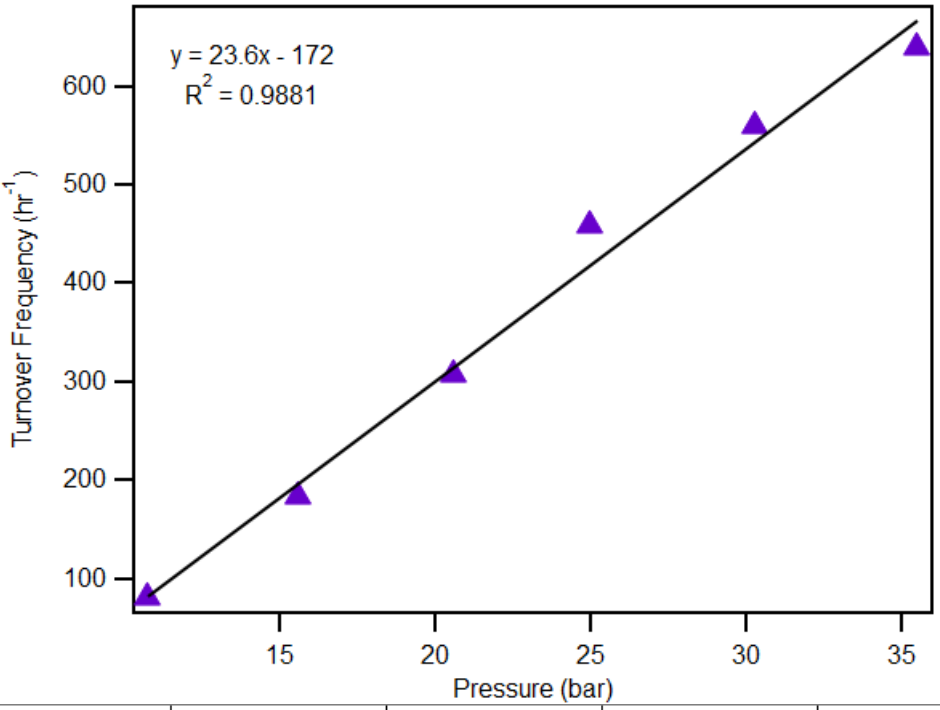

Pressure (bar)	TON MeOAc	TON AcOH	Total TON	TOF(hr-1)
10.78	194	47	241	80
15.62	408	139	547	182
20.64	720	199	919	306
25	1011	360	1371	457
30.3	1271	407	1678	559
35.5	1192	723	1915	638

Figure S24. CO pressure dependence of methanol carbonylation reaction with **2**^{18c6}. Conditions: 150 °C, 3 hours and 0.34 mM [Ir] with 0.5 M CH_3I.

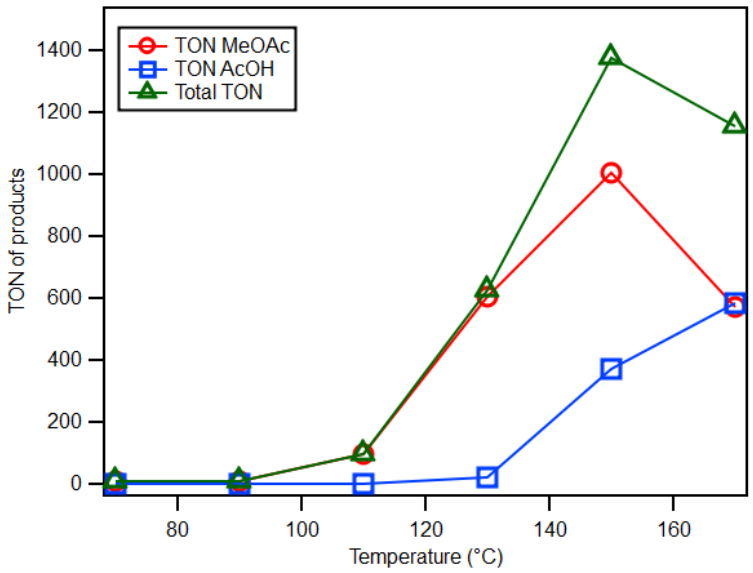

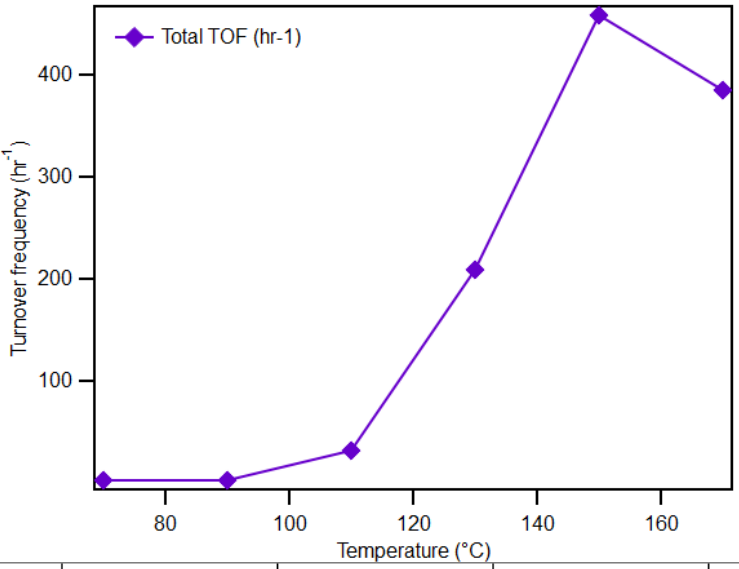

Temperature	TON MeOAc	TON AcOH	Total TON	TOF (hr-1)
70	7	0	7	2.37119
90	8	0	8	2.62393
110	96	0	96	31.8806
130	606	20	626	208.726
150	1004	370	1375	458.188
170	572	583	1155	385.118

Figure S25. Temperature dependence of methanol carbonylation reaction with $\mathbf{2}^{\mathbf{18c6}}$. Conditions: 3 hours, 25 bar and 0.34 mM [Ir] with 0.5 M CH_3I.

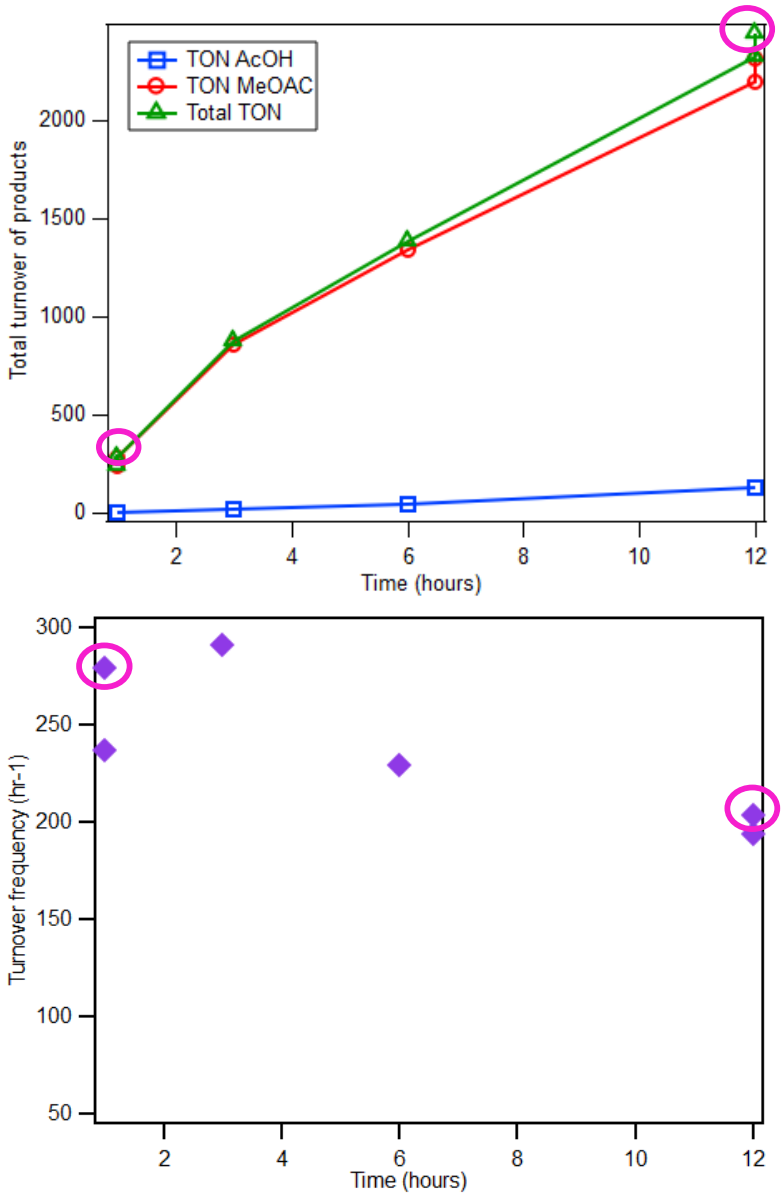

Hours	additive	TON_MeOAC	TON_AcOH	Total_TON	TOF
1		237	0	237	236.674
1	10	279	0	279	279.416
3		857	15	872	290.674
6		1336	41	1377	229.461
12		2195	128	2323	193.548
12	10	2317	123	2440	203.313

Figure S26. Turnover frequency of methanol carbonylation with **2**^{18c6} at different reaction times. Conditions: 25 bar and 0.34 mM [Ir] with 0.1 M CH_3I at 150 ºC. Data points circled in pink contained 10 equivalents (3.4 mM) of [TBA][I].

Table S1. Lewis acid screening with (^{18c6}NCOP^{iPr})Ir(CO) (**2**^{18c6})[a]

Lewis acid Salt[a]	TON CH_3OAc	TON AcOH	Total TON	Promotion Factor[b]
$La(OTf)_3$	510	10	520	0.53
LaI_3	680	10	690	0.70
$CeCl_3$	680	30	710	0.73
$Ce(OTf)_3$	760	30	790	0.81
GaI_3	900	20	920	0.94
No additive	940	40	980	-
NaCl	1040	30	1070	1.09
$HfCl_4$	1080	30	1110	1.13
$ZrCl_4$	1090	40	1130	1.15
KCl	1110	40	1150	1.18
LiCl	1150	40	1190	1.21

[a] Conditions: 150 °C, 25 bar CO, 3 h, 0.1 M CH_3I, 0.34 mM Ir catalyst, 0.34 mM Lewis acid.
[b] Calculated as a ratio of total TON/TON with no Lewis acid present.

Table S2. Electrolyte screening with (^{18c6}NCOP^{iPr})Ir(CO) (**2**^{18c6})[a]

Electrolyte	TON CH_3OAc	TON AcOH	Total TON	Promotion Factor[b]
No additive	940	40	980	-
[TBA][OTf]	970	20	990	1.01
[TBA][I]	1430	40	1470	1.50

[a]Conditions: 150 °C, 25 bar CO, 3 hr, 0.1 M CH_3I, 0.34 mM Ir catalyst, 3.4 mM electrolyte.
[b]Calculated as a ratio of total TON/TON with no Lewis acid present.

Table S3. Catalytic runs with both Lewis Acid salts and added Electrolyte with (^{18c6}NCOP^{iPr})Ir(CO) (**2**^{18c6}).[a]

Electrolyte	Salt	TON CH_3OAc	TON AcOH	Total TON	Promotion Factor[b]
[TBA][OTf]	$LaOTf_3$	900	20	920	0.94
[TBA][OTf]	LaI_3	930	20	950	0.97
None	None	940	40	980	-
[TBA][OTf]	None	970	20	990	1.01
[TBA][OTf]	$ZrCl_4$	1200	20	1220	1.24
[TBA][OTf]	$Ce(OTf)_3$	1210	20	1230	1.26
[TBA][OTf]	LiCl	1250	10	1260	1.29
[TBA][OTf]	$HfCl_4$	1270	40	1310	1.34
[TBA][OTf][c]	$HfCl_4$	1540	40	1580	1.61

[a]Conditions: 150 °C, 25 bar CO, 3 hr, 0.1 M CH_3I, 0.34 mM Ir catalyst, 3.4 mM electrolyte, 0.34 mM salt.
[b]Calculated as a ratio of total TON/TON with no Lewis acid or electrolyte present.
[c]Catalyst formed in situ from [PPN][$Ir(CO)_2I_2$] and (^{18c6}NCOP^{iPr})H.

Table S4. Lewis acid screening with ($^{MeO\text{-}18c6}$NCOP^{iPr})Ir(CO) (**2**$^{\mathbf{MeO\text{-}18c6}}$)[a]

Lewis acid	TON CH_3OAc	TON AcOH	Total TON	Promotion Factor[b]
$ZrCl_4$	520	10	530	0.35
LaI_3	660	20	680	0.45
$La(OTf)_3$	670	10	680	0.45
GaI_3	1220	40	1260	0.84
LiCl	1240	20	1260	0.84
[TBA][I]	1280	30	1320	0.88
$HfCl_4$	1290	40	1330	0.88
None	1450	50	1500	-
[TBA][OTf]	1630	40	1670	1.11
[TBA][Cl]	1650	40	1690	1.13

[a]Conditions: 150 °C, 25 bar CO, 3 hr, 0.1 M CH_3I, 0.34 mM Ir catalyst, 3.4 mM electrolyte, 0.34 mM Lewis acid.
[b]Calculated as a ratio of total TON/TON with no Lewis acid.

Table S5. Lewis acid screening with ($^{MeO\text{-}15c5}$NCOP^{iPr})Ir(CO) (**2**$^{\mathbf{MeO\text{-}15c5}}$)[a]

Lewis Acid	TON CH_3OAc	TON AcOH	Total TON	Promotion Factor[b]
$La(OTf)_3$	790	5	795	0.81
LaI_3	820	20	840	0.87
$ZrCl_4$	950	10	960	0.99
None	970	0	970	-
GaI_3	1020	10	1030	1.06
$HfCl_4$	1230	20	1250	1.29
[TBA][OTf]	1300	40	1340	1.38
LiCl	1560	50	1610	1.66
[TBA][I]	1720	20	1740	1.80
[TBA][Cl]	1940	10	1950	2.01

[a]Conditions: 150 °C, 25 bar CO, 3 hr, 0.1 M CH_3I, 0.34 mM Ir catalyst, 3.4 mM electrolyte, and 0.34 mM Lewis acid.
[b]Calculated as a ratio of total TON/TON with no Lewis acid.

Table S6. Catalytic methanol carbonylation by [PPN][$Ir(CO)_2I_2$] under standard conditions

Lewis acid	TON CH_3OAc	TON AcOH	Total TON	Promotion Factor[b]
None	1800	70	1870	–
LiCl	2220	180	2400	1.28
[TBA][I]	1800	70	1870	1.00

[a]Conditions: 150 °C, 25 bar CO, 3 hr, 0.1 M CH_3I, 0.34 mM Ir catalyst, 0.34 mM Lewis acid.
[b]Calculated as a ratio of total TON/TON with no Lewis acid.

III. NMR Studies: Catalyst Speciation and Turnover Under Various Conditions

A. Catalysis speciation after reactor runs

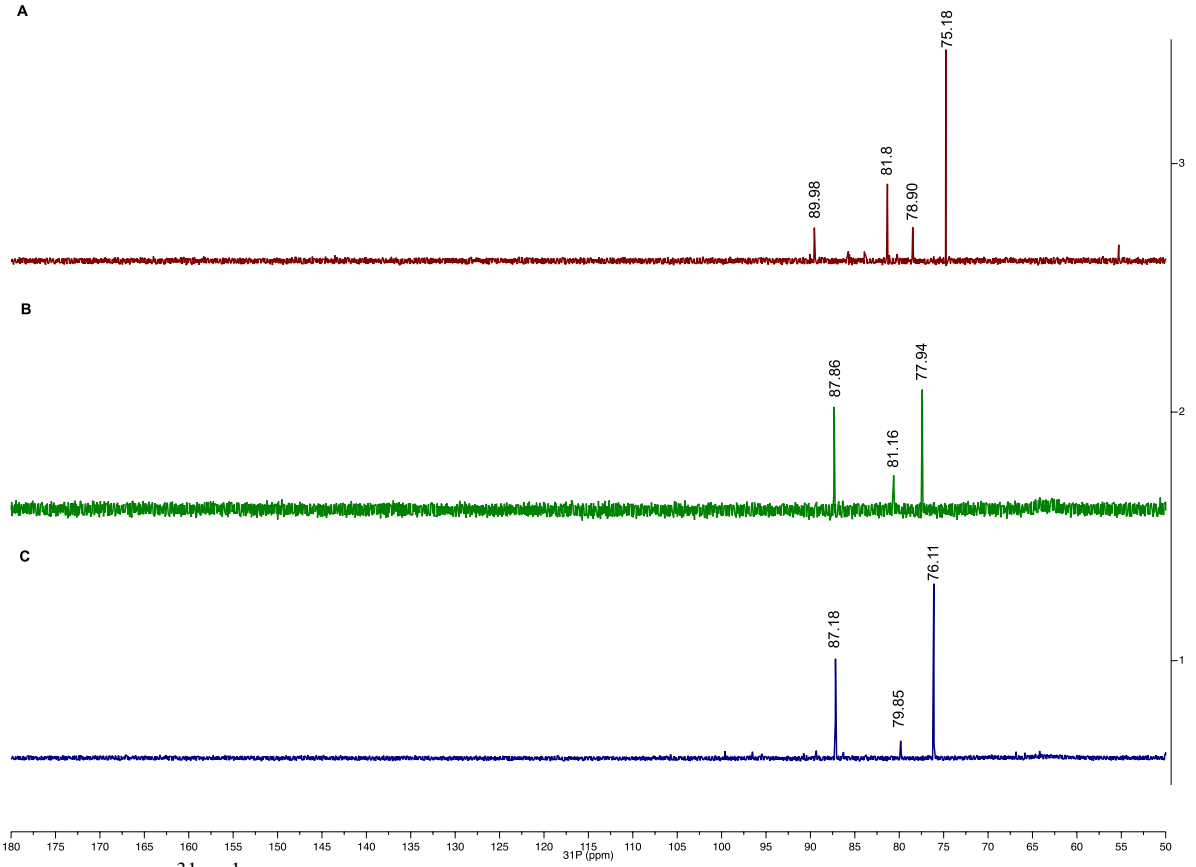

Figure S27. $^{31}P\{^{1}H\}$ NMR spectra of the reaction mixture following methanol carbonylation catalysis in the presence of 0.1 M CH_3I at 25 bar CO for 3 h using (^{18c6}NCOP^{iPr})Ir(CO) (**2**$^{\mathbf{18c6}}$) at 130 ºC (A), ($^{MeO\text{-}15c5}$NCOP^{iPr})Ir(CO) (**2**$^{\mathbf{MeO\text{-}15c5}}$) and 1 equiv LiCl at 150 ºC (B), and ($^{MeO\text{-}18c6}$NCOP^{iPr})Ir(CO) (**2**$^{\mathbf{MeO\text{-}18c6}}$) at 150 ºC (C).

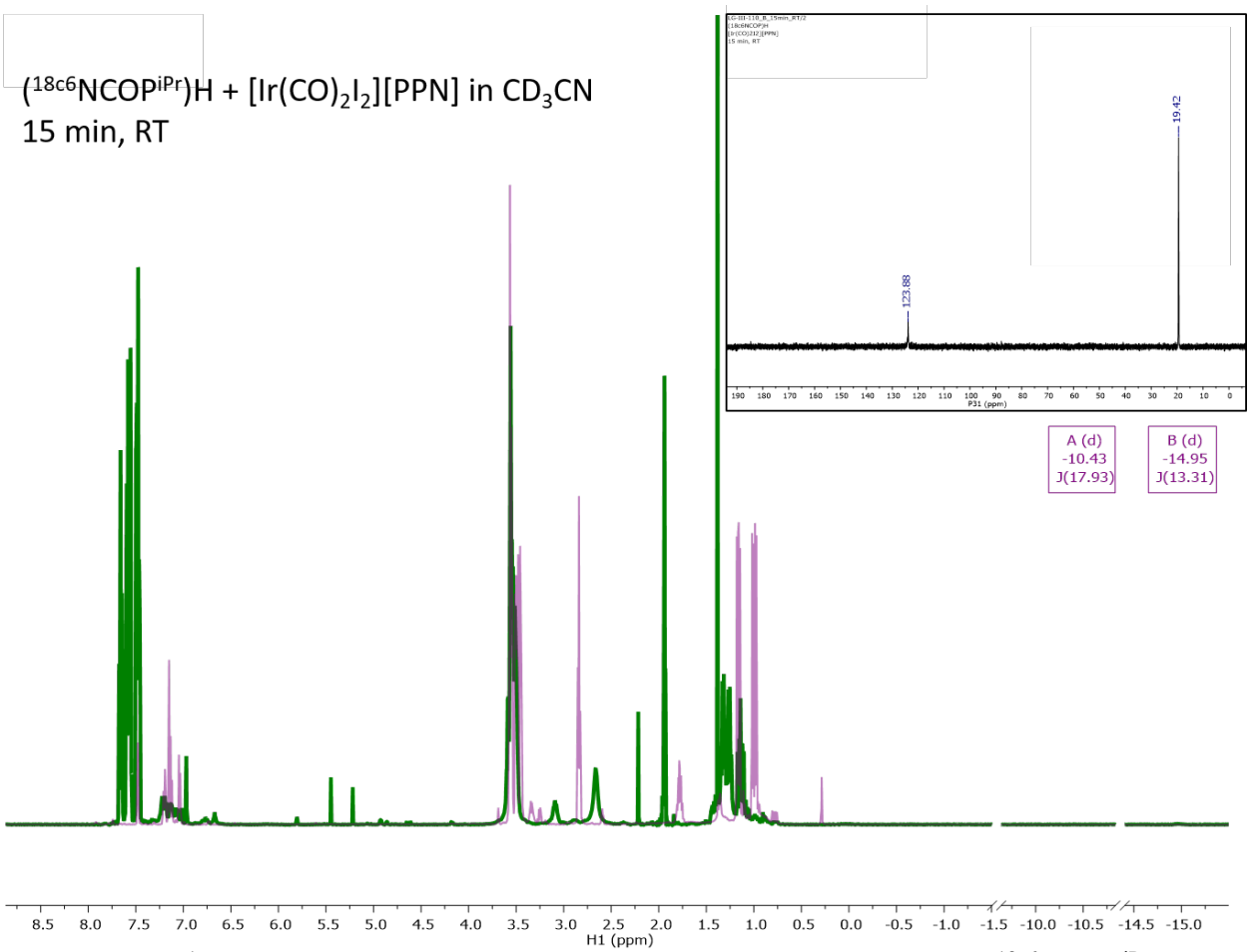

Figure S28. ^{1}H NMR spectrum of the product formed after mixing (^{18c6}NCOP^{iPr})H and [PPN][Ir(CO)$_2$I$_2$] in CD_3CN (green) overlayed with a spectrum of free ligand (^{18c6}NCOP^{iPr})H (purple). Shifts in the isopropyl protons (δ 1.0-1.5) are indicative of coordination of the phosphine to the iridium center. Inset: ^{31}P{^{1}H} NMR shows formation of a single major product (δ 124) along with [PPN]$^{+}$ (δ 19).

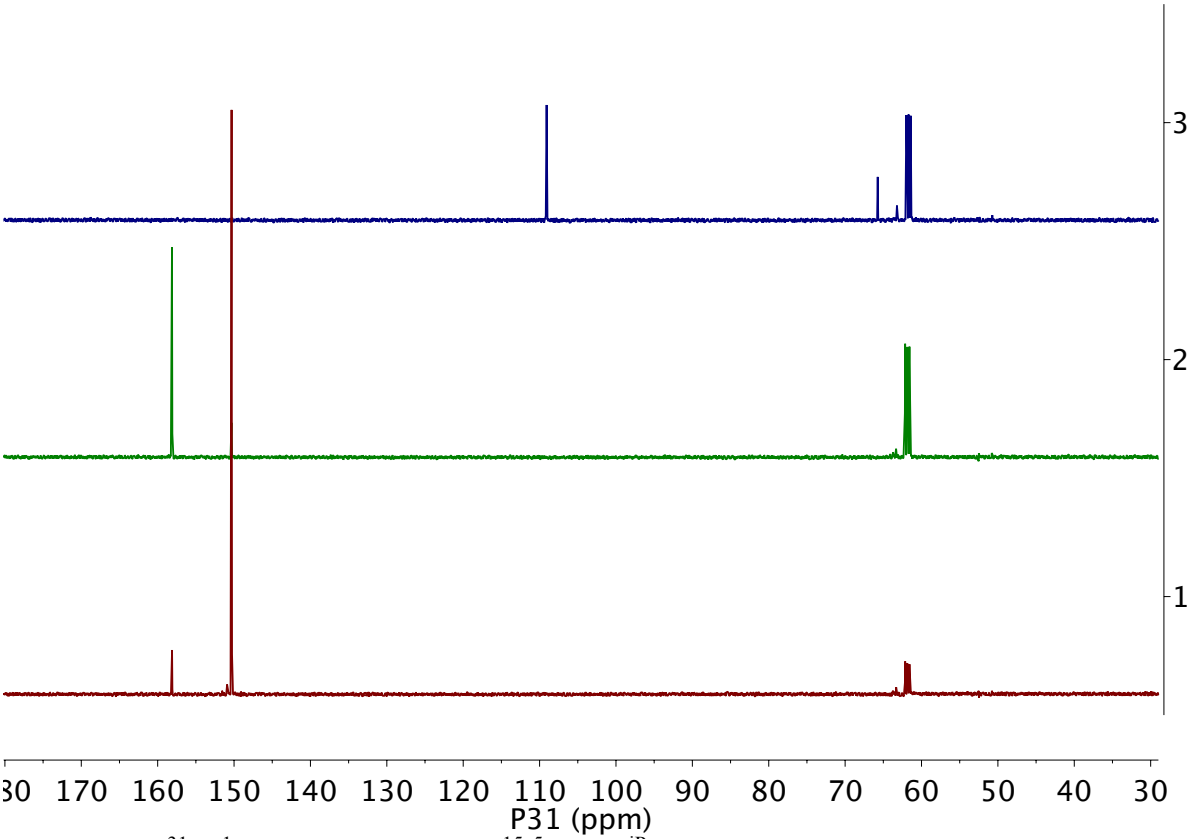

Figure S29. $^{31}P\{^{1}H\}$ NMR spectra of ($^{15c5}NCOP^{iPr}$)H in CD_3OD after 0.5 h (bottom red trace), 22 h (middle green trace), and after addition of 35 μL CH_3I (top blue trace). The species are tentatively assigned as follows: ($^{15c5}NCOP^{iPr}$)H (δ 147), *i*Pr_2POCD_3 (δ 158), *i*$Pr_2P(O)D$ (δ 61.8, 1:1:1 t, J_{PD} = 68 Hz), [*i*$Pr_2P(CH_3)(OCH_3)$]$^+$ (δ 109).

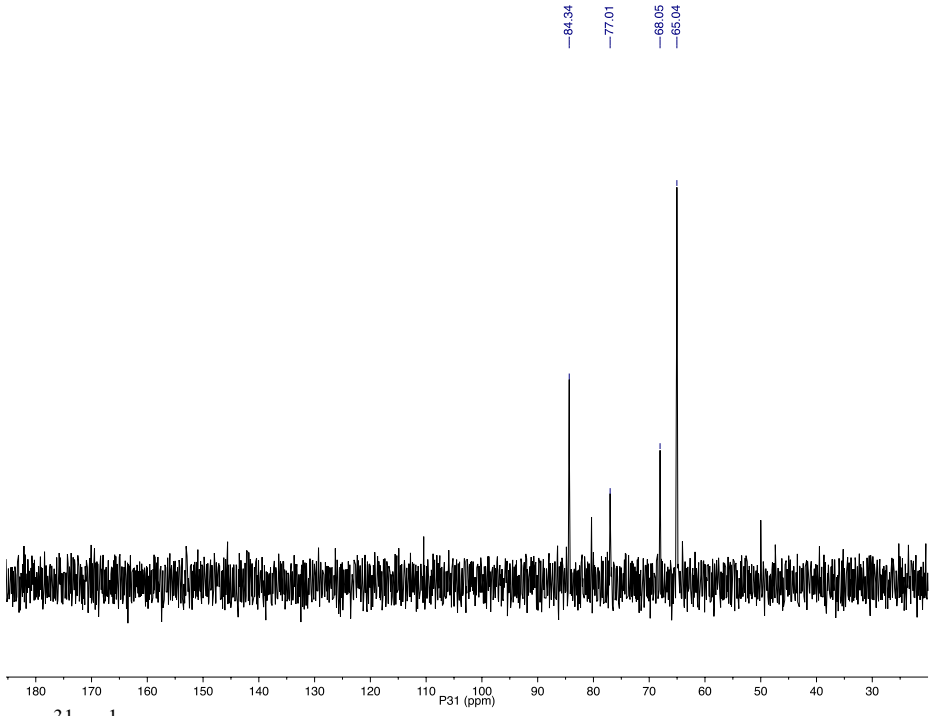

Figure S30. $^{31}P\{^{1}H\}$ NMR spectrum after carbonylation reaction using 2.5 mM (^{18c6}NCOP^{iPr})Ir(CO) and 0.74 mM MeI pressurized with 25 bar CO and heated to 150 °C for 6 h.

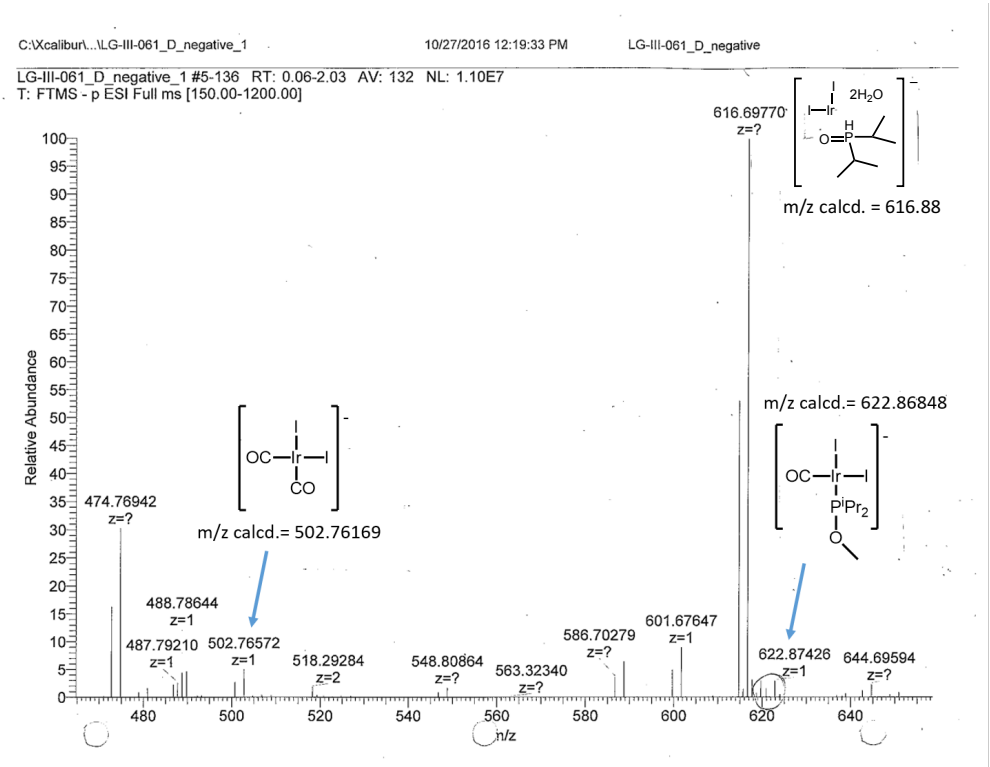

Figure S31. Electrospray mass spectrometry after carbonylation reaction using 2.5 mM (^{18c6}NCOP^{iPr})Ir(CO) and 0.74 mM MeI pressurized with 25 bar CO and heated to 150 °C for 6 h.

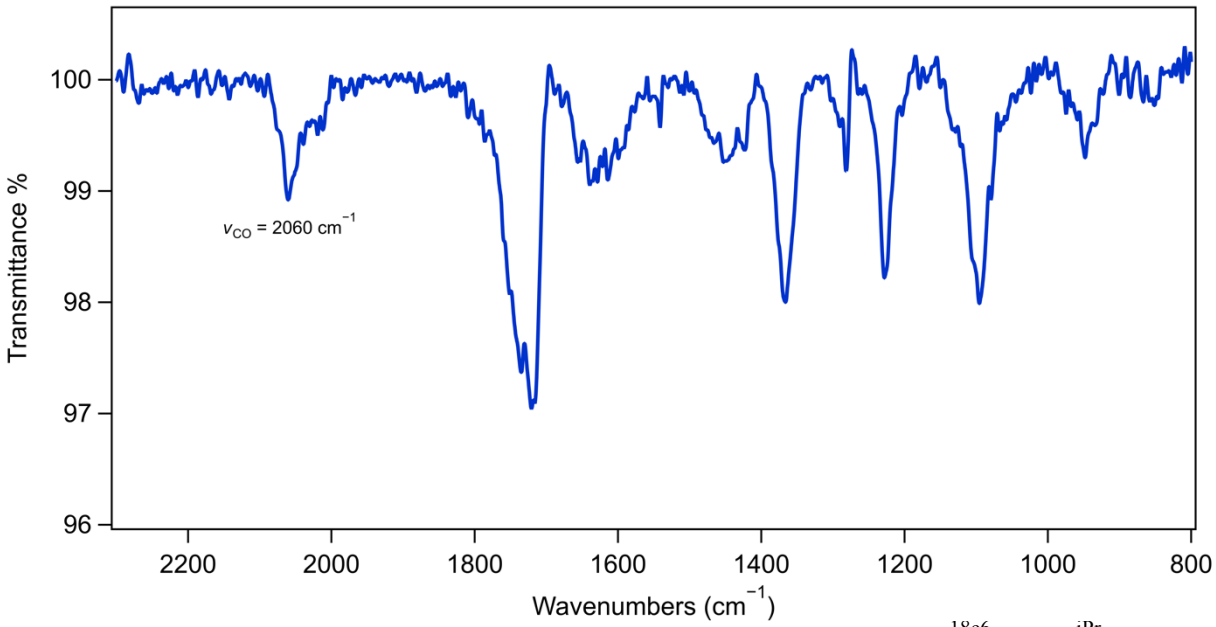

Figure S32. Infrared spectrum after carbonylation reaction using 2.5 mM (^{18c6}NCOP^{iPr})Ir(CO) and 0.74 mM MeI pressurized with 25 bar CO and heated to 150 °C for 6 h.

B. Representative spectra of NMR-scale catalysis at low temperature and low pressure

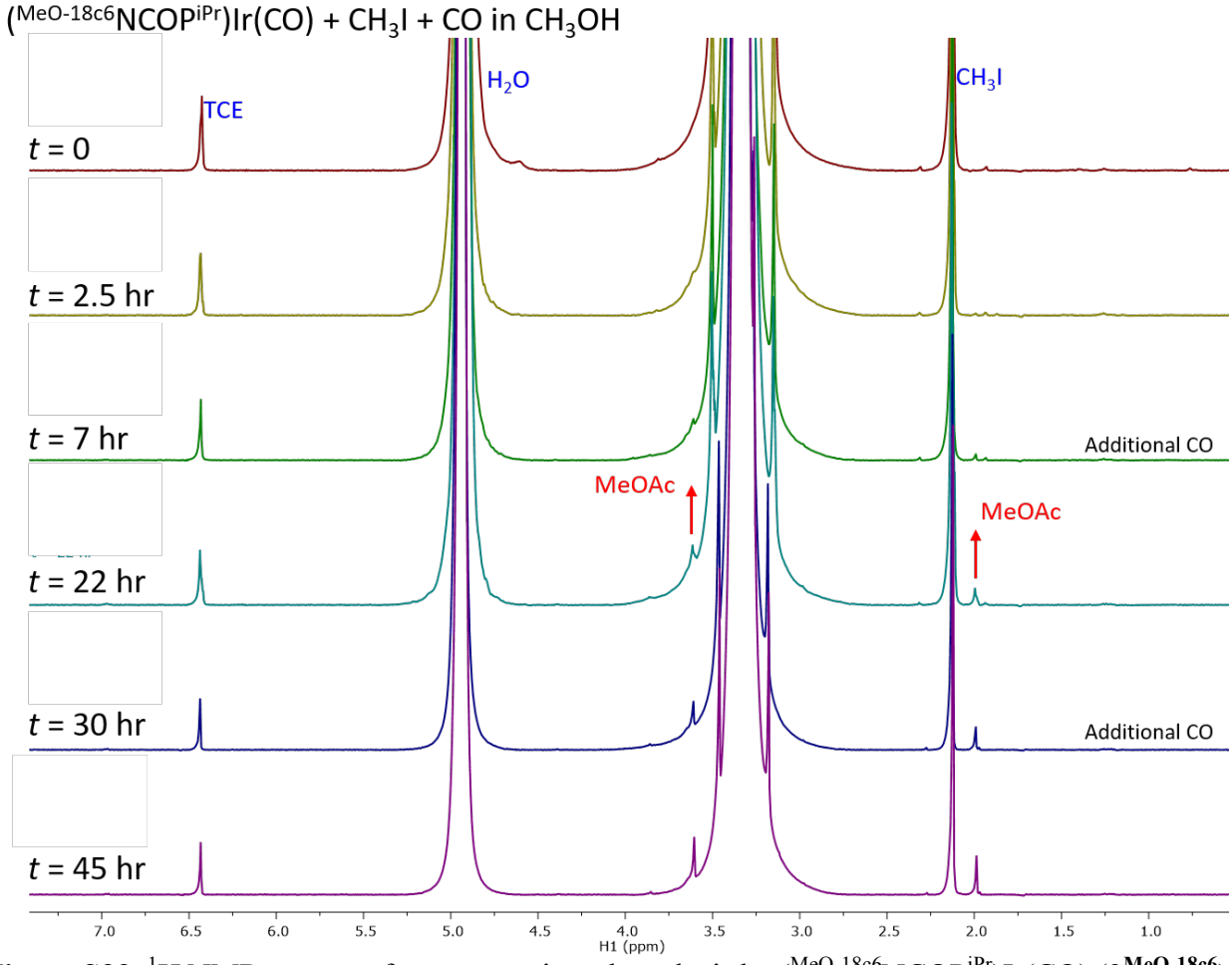

Figure S33. ^{1}H NMR spectra of *in situ* monitored catalysis by ($^{MeO\text{-}18c6}$NCOP^{iPr})Ir(CO) (**2**$^{\mathbf{MeO\text{-}18c6}}$) at low temperature (70 °C) and pressure (1 bar CO). 1,1,2,2-tetrachloroethane (TCE) was used as an internal standard and the growth of CH_3OAc can be seen at 2.0 and 3.6 ppm.

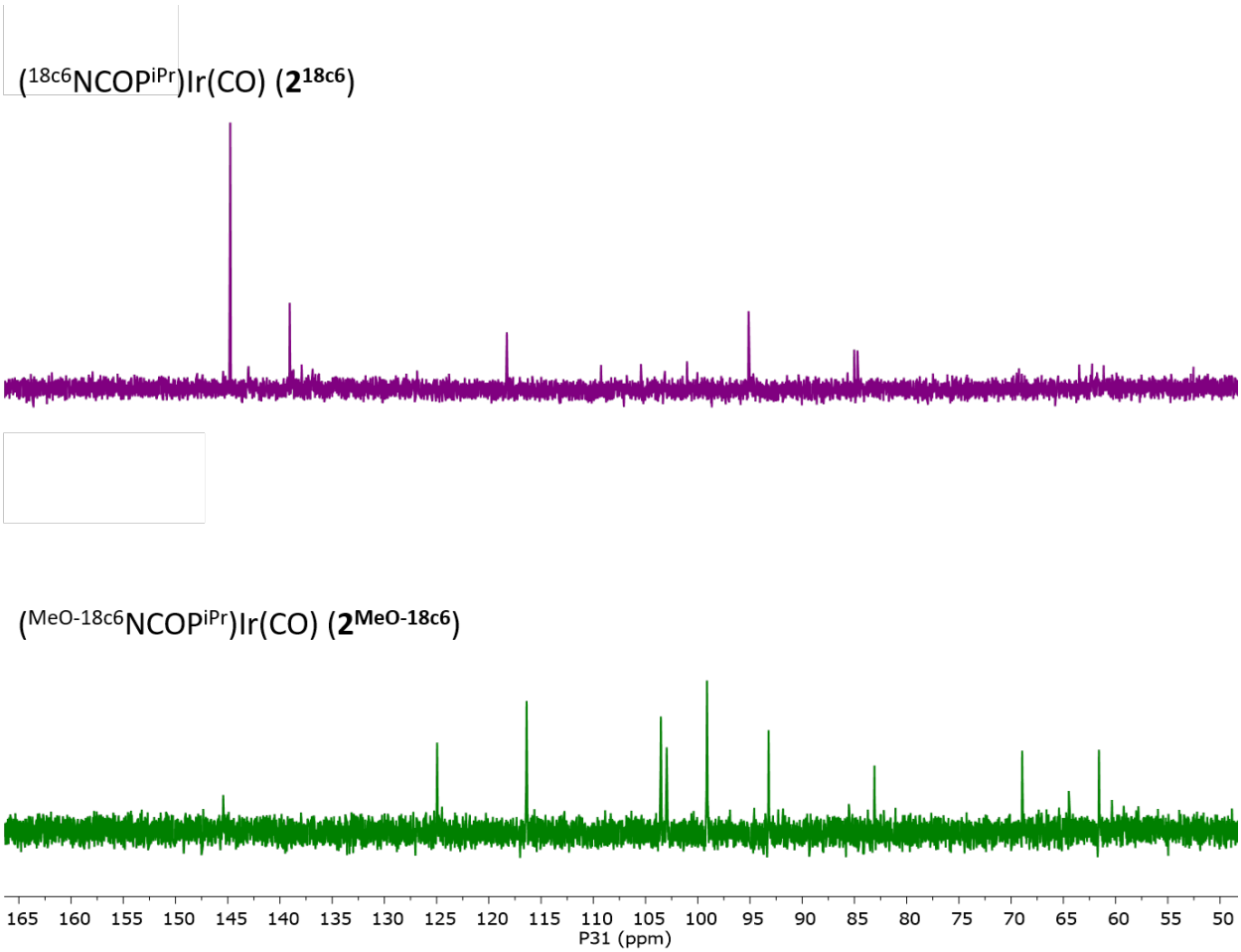

Figure S34. $^{31}P\{^{1}H\}$ NMR spectra of final products after 40 h of catalysis at low temperature (70 °C) and pressure (1 bar CO) for both iridium pincer catalysts.

C. Stoichiometric reactivity monitored by NMR spectroscopy

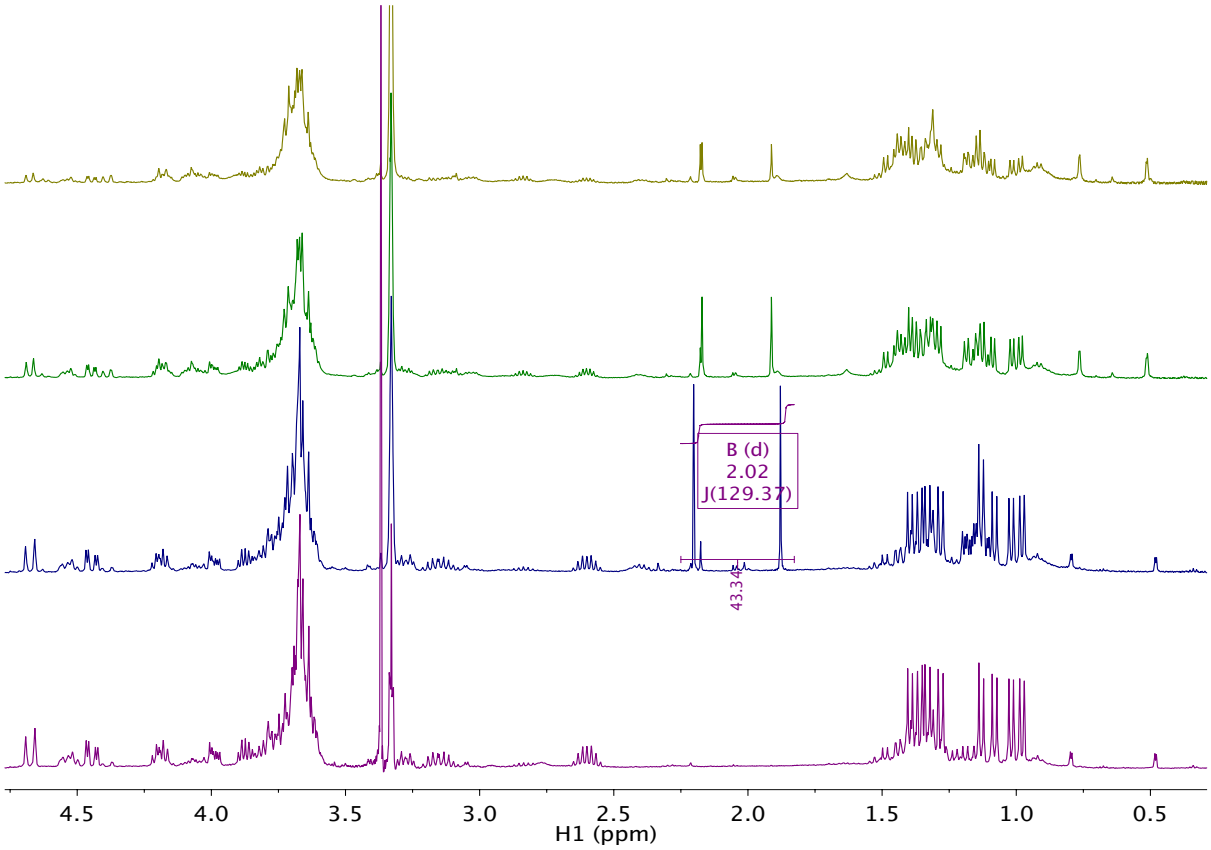

Figure S35. ^{1}H NMR spectra of (^{15c5}NCOP^{iPr})Ir(^{13}CH$_3$)(CO)(I) under 1 atm CO in CD$_3$OH utilizing a CD$_3$OD capillary tube at 2 h (top), 4 h (upper middle), and 40 h (lower middle). The presence of free methyl acetate was confirmed by evaporation of the reaction solvent and re-dissolving in fresh CD$_3$OD (bottom), which removes the volatile product.

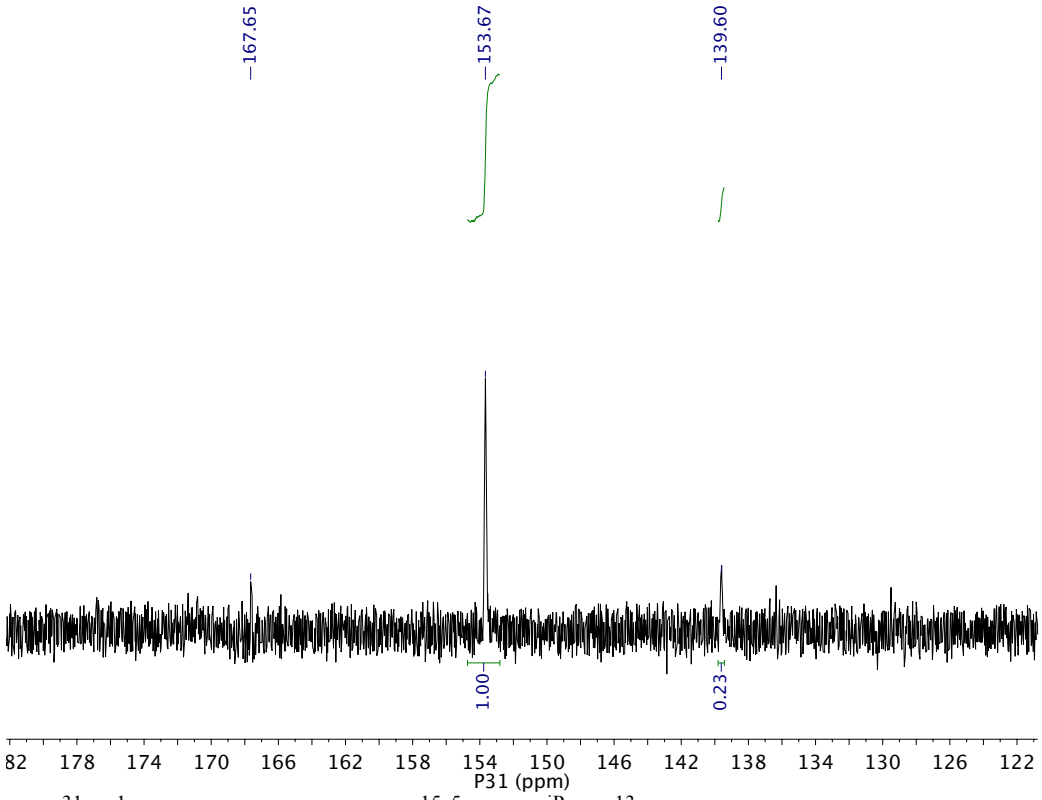

Figure S36. $^{31}P\{^{1}H\}$ NMR spectrum of ($^{15c5}NCOP^{iPr}$)Ir($^{13}CH_3$)(CO)(I) under 1 atm CO in CD_3OD after 40 h.

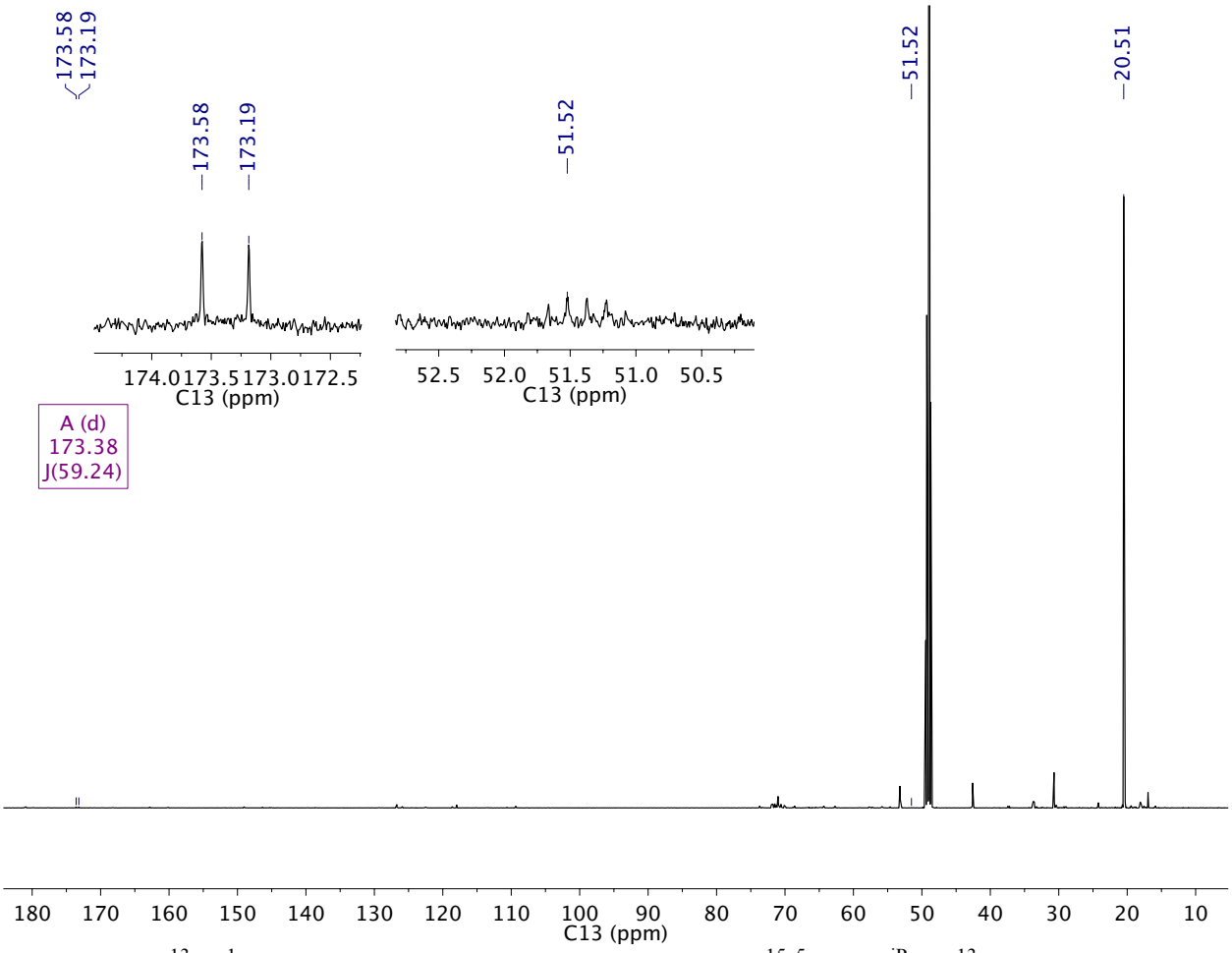

Figure S37. $^{13}C\{^{1}H\}$ NMR spectrum after the reaction of ($^{15c5}NCOP^{iPr}$)Ir($^{13}CH_3$)(CO)(I) with 1 atm CO in CD_3OD. Highlighted resonances are consistent with $^{13}CH_3C(O)OCD_3$.

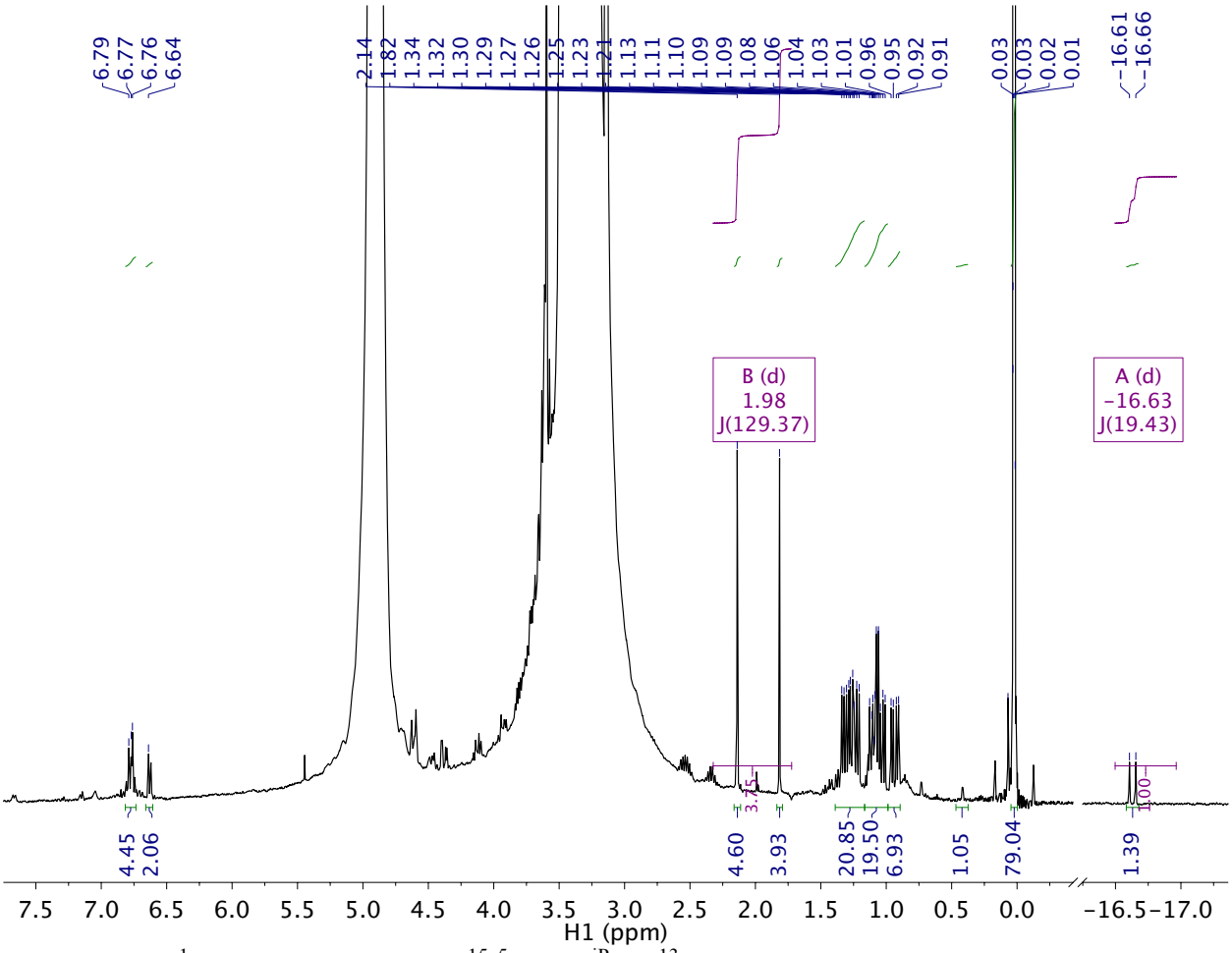

Figure S38. ^{1}H NMR spectra of (^{15c5}NCOP^{iPr})Ir(^{13}CH$_3$)(CO)(I) under 1 atm CO in CH$_3$OH utilizing a CD$_3$OD capillary tube after 40 h.

IV. Crystallographic Details

Table S7. Crystal data and structure refinement for (^{18c6}NCOP^{iPr})Ir(H)(CO)(Cl) ($\mathbf{1}^{18c6}$).

Identification code	x1510003
Empirical formula	$C_{26}H_{44}ClIrNO_7P$
Formula weight	741.24
Temperature/K	100.15
Crystal system	monoclinic
Space group	$P2_1/c$
a/Å	15.0632(4)
b/Å	12.3425(3)
c/Å	16.2371(4)
α/°	90
β/°	107.6431(13)
γ/°	90
Volume/Å^3	2876.77(13)
Z	4
ρ_{calc}g/cm^3	1.711
μ/mm^{-1}	10.732
F(000)	1488.0
Crystal size/mm^3	0.155 × 0.061 × 0.051
Radiation	CuKα (λ = 1.54178)
2Θ range for data collection/°	6.156 to 140.38
Index ranges	$-18 \le h \le 18$, $-15 \le k \le 15$, $-19 \le l \le 19$
Reflections collected	53983
Independent reflections	51638 [R_{int} = 0.0456, R_{sigma} = 0.0407]
Data/restraints/parameters	51638/0/343
Goodness-of-fit on F^2	1.026
Final R indexes [I>=2σ (I)]	R_1 = 0.0385, wR_2 = 0.0882
Final R indexes [all data]	R_1 = 0.0495, wR_2 = 0.0936
Largest diff. peak/hole / e Å^{-3}	1.28/-0.70

Table S8. Bond Lengths for (^{18c6}NCOP^{iPr})Ir(H)(CO)(Cl) ($\mathbf{1}^{18c6}$).

Atom	Atom	Length/Å	Atom	Atom	Length/Å
Ir1	Cl1	2.5070(13)	C15	C16	1.511(8)
Ir1	P1	2.2288(13)	C16	N17	1.513(7)
Ir1	C1	1.933(6)	N17	C18	1.509(7)
Ir1	C10	2.030(6)	N17	C34	1.507(7)
Ir1	N17	2.224(5)	C18	C19	1.523(8)
P1	C3	1.832(6)	C19	O20	1.427(7)

P1	C6	1.826(6)	O20	C21	1.422(7)
P1	O9	1.658(4)	C21	C22	1.504(8)
C1	O2	1.130(8)	C22	O23	1.424(7)
C3	C4	1.531(8)	O23	C24	1.425(7)
C3	C5	1.529(8)	C24	C25	1.506(9)
C6	C7	1.534(7)	C25	O26	1.424(7)
C6	C8	1.529(8)	O26	C27	1.415(8)
O9	C11	1.399(7)	C27	C28	1.501(9)
C10	C11	1.385(8)	C28	O29	1.427(7)
C10	C15	1.393(8)	O29	C30	1.416(7)
C11	C12	1.381(9)	C30	C31	1.505(8)
C12	C13	1.399(9)	C31	O32	1.415(7)
C13	C14	1.393(9)	O32	C33	1.432(7)
C14	C15	1.392(9)	C33	C34	1.521(8)

Table S9. Bond Angles for (^{18c6}NCOP^{iPr})Ir(H)(CO)(Cl) (1^{18c6}).

Atom	Atom	Atom	Angle/°	Atom	Atom	Atom	Angle/°
P1	Ir1	Cl1	97.86(5)	C11	C12	C13	117.3(6)
C1	Ir1	Cl1	94.53(17)	C14	C13	C12	121.6(6)
C1	Ir1	P1	98.56(17)	C15	C14	C13	119.5(6)
C1	Ir1	C10	176.0(2)	C10	C15	C16	114.1(5)
C1	Ir1	N17	102.4(2)	C14	C15	C10	119.6(6)
C10	Ir1	Cl1	89.25(16)	C14	C15	C16	126.1(6)
C10	Ir1	P1	79.51(16)	C15	C16	N17	110.3(5)
C10	Ir1	N17	79.1(2)	C16	N17	Ir1	105.9(3)
N17	Ir1	Cl1	88.13(12)	C18	N17	Ir1	112.0(3)
N17	Ir1	P1	157.68(14)	C18	N17	C16	106.1(5)
C3	P1	Ir1	119.14(19)	C34	N17	Ir1	110.7(4)
C6	P1	Ir1	118.73(19)	C34	N17	C16	109.4(4)
C6	P1	C3	107.8(3)	C34	N17	C18	112.4(4)
O9	P1	Ir1	106.69(15)	N17	C18	C19	116.0(5)
O9	P1	C3	99.3(2)	O20	C19	C18	109.8(5)
O9	P1	C6	101.8(2)	C21	O20	C19	112.5(5)
O2	C1	Ir1	175.1(5)	O20	C21	C22	115.1(5)
C4	C3	P1	110.0(4)	O23	C22	C21	109.0(5)
C5	C3	P1	113.1(4)	C22	O23	C24	112.7(5)
C5	C3	C4	111.6(5)	O23	C24	C25	113.2(5)
C7	C6	P1	113.3(4)	O26	C25	C24	111.4(5)
C8	C6	P1	111.2(4)	C27	O26	C25	110.0(5)
C8	C6	C7	112.7(5)	O26	C27	C28	110.9(5)
C11	O9	P1	114.4(3)	O29	C28	C27	110.4(5)

C11	C10	Ir1	122.1(4)	C30	O29	C28	110.8(5)
C11	C10	C15	119.5(5)	O29	C30	C31	110.7(5)
C15	C10	Ir1	118.4(4)	O32	C31	C30	109.8(5)
C10	C11	O9	117.0(5)	C31	O32	C33	111.8(4)
C12	C11	O9	120.6(5)	O32	C33	C34	108.6(5)
C12	C11	C10	122.3(6)	N17	C34	C33	116.7(5)

Table S10. Torsion Angles for (^{18c6}NCOP^{iPr})Ir(H)(CO)(Cl) ($\mathbf{1}^{18c6}$).

A	B	C	D	Angle/°	A	B	C	D	Angle/°
Ir1	P1	C3	C4	-51.7(5)	C12	C13	C14	C15	1.3(9)
Ir1	P1	C3	C5	73.8(5)	C13	C14	C15	C10	2.3(9)
Ir1	P1	C6	C7	-179.5(4)	C13	C14	C15	C16	-173.2(5)
Ir1	P1	C6	C8	-51.3(5)	C14	C15	C16	N17	-152.4(5)
Ir1	P1	O9	C11	-4.2(4)	C15	C10	C11	O9	-177.9(5)
Ir1	C10	C11	O9	2.9(7)	C15	C10	C11	C12	2.6(9)
Ir1	C10	C11	C12	-176.6(4)	C15	C16	N17	Ir1	-36.9(5)
Ir1	C10	C15	C14	175.0(4)	C15	C16	N17	C18	82.2(5)
Ir1	C10	C15	C16	-9.0(7)	C15	C16	N17	C34	-156.3(5)
Ir1	N17	C18	C19	-63.2(5)	C16	N17	C18	C19	-178.3(4)
Ir1	N17	C34	C33	178.1(4)	C16	N17	C34	C33	-65.5(6)
P1	O9	C11	C10	1.3(6)	N17	C18	C19	O20	104.5(6)
P1	O9	C11	C12	-179.2(4)	C18	N17	C34	C33	52.1(6)
C3	P1	C6	C7	-40.1(5)	C18	C19	O20	C21	-161.1(5)
C3	P1	C6	C8	88.2(4)	C19	O20	C21	C22	-73.4(6)
C3	P1	O9	C11	-128.5(4)	O20	C21	C22	O23	-73.6(6)
C6	P1	C3	C4	169.0(4)	C21	C22	O23	C24	169.8(5)
C6	P1	C3	C5	-65.5(5)	C22	O23	C24	C25	-88.4(6)
C6	P1	O9	C11	120.9(4)	O23	C24	C25	O26	70.3(7)
O9	P1	C3	C4	63.4(4)	C24	C25	O26	C27	-176.1(5)
O9	P1	C3	C5	-171.1(4)	C25	O26	C27	C28	-175.2(5)
O9	P1	C6	C7	63.8(5)	O26	C27	C28	O29	-74.0(7)
O9	P1	C6	C8	-167.9(4)	C27	C28	O29	C30	174.3(5)
O9	C11	C12	C13	-178.5(5)	C28	O29	C30	C31	168.1(5)
C10	C11	C12	C13	0.9(9)	O29	C30	C31	O32	63.9(7)
C10	C15	C16	N17	32.0(7)	C30	C31	O32	C33	178.7(5)
C11	C10	C15	C14	-4.2(8)	C31	O32	C33	C34	167.4(5)
C11	C10	C15	C16	171.8(5)	O32	C33	C34	N17	-80.9(6)
C11	C12	C13	C14	-2.9(9)	C34	N17	C18	C19	62.2(6)

Table S11. Crystal data and structure refinement for (^{18c6}NCOP^{iPr})Ir(CO) (2^{18c6}).

Identification code	x1509008
Empirical formula	$C_{26}H_{43}IrNO_7P$
Formula weight	704.78
Temperature/K	100
Crystal system	triclinic
Space group	P-1
a/Å	7.7588(6)
b/Å	15.5942(12)
c/Å	24.1160(19)
α/°	89.185(4)
β/°	82.743(4)
γ/°	89.582(5)
Volume/Å^3	2894.1(4)
Z	4
ρ_{calc}g/cm^3	1.618
μ/mm^{-1}	9.806
F(000)	1416.0
Crystal size/mm^3	0.199 × 0.195 × 0.094
Radiation	CuKα (λ = 1.54178)
2Θ range for data collection/°	3.694 to 144.548
Index ranges	$-9 \le h \le 9$, $-19 \le k \le 19$, $-29 \le l \le 29$
Reflections collected	114739
Independent reflections	11097 [R_{int} = 0.0466, R_{sigma} = 0.0269]
Data/restraints/parameters	11097/0/657
Goodness-of-fit on F^2	1.068
Final R indexes [I>=2σ (I)]	R_1 = 0.0246, wR_2 = 0.0511
Final R indexes [all data]	R_1 = 0.0299, wR_2 = 0.0526
Largest diff. peak/hole / e Å^{-3}	0.51/-0.76

Table S12. Bond Angles for (^{18c6}NCOP^{iPr})Ir(CO) (2^{18c6}).

Atom	Atom	Atom	Angle/°	Atom	Atom	Atom	Angle/°
C9	Ir1	P2	100.73(10)	C43	Ir2	P3	100.27(9)
C9	Ir1	C17	178.77(12)	C43	Ir2	C51	177.99(12)
C9	Ir1	N19	100.69(11)	C43	Ir2	N53	102.64(11)
C17	Ir1	P2	79.78(9)	C51	Ir2	P3	79.08(9)

C17	Ir1	N19	78.62(11)	C51	Ir2	N53	78.21(11)
N19	Ir1	P2	156.44(6)	N53	Ir2	P3	156.37(6)
C3	P2	Ir1	116.74(11)	C37	P3	Ir2	118.57(11)
C3	P2	C6	106.17(14)	C37	P3	C40	105.73(14)
C6	P2	Ir1	123.40(10)	C40	P3	Ir2	121.98(10)
O11	P2	Ir1	107.43(8)	O45	P3	Ir2	107.30(8)
O11	P2	C3	99.88(13)	O45	P3	C37	99.99(13)
O11	P2	C6	99.17(12)	O45	P3	C40	99.25(12)
C4	C3	P2	109.3(2)	C38	C37	P3	111.1(2)
C5	C3	P2	110.6(2)	C38	C37	C39	111.4(3)
C5	C3	C4	111.5(3)	C39	C37	P3	109.4(2)
C7	C6	P2	108.4(2)	C41	C40	P3	112.8(2)
C7	C6	C8	111.4(3)	C42	C40	P3	107.9(2)
C8	C6	P2	113.5(2)	C42	C40	C41	111.5(3)
O10	C9	Ir1	178.5(3)	O44	C43	Ir2	178.6(3)
C12	O11	P2	113.63(18)	C46	O45	P3	113.13(18)
C13	C12	O11	120.7(3)	C47	C46	O45	121.4(3)
C13	C12	C17	122.2(3)	C47	C46	C51	122.2(3)
C17	C12	O11	117.1(3)	C51	C46	O45	116.4(3)
C12	C13	C14	117.3(3)	C46	C47	C48	117.4(3)
C15	C14	C13	122.1(3)	C49	C48	C47	122.2(3)
C14	C15	C16	119.2(3)	C48	C49	C50	118.8(3)
C15	C16	C18	125.1(3)	C49	C50	C51	120.2(3)
C17	C16	C15	119.9(3)	C49	C50	C52	125.4(3)
C17	C16	C18	115.0(3)	C51	C50	C52	114.5(3)
C12	C17	Ir1	121.7(2)	C46	C51	Ir2	122.3(2)
C16	C17	Ir1	118.9(2)	C46	C51	C50	119.2(3)
C16	C17	C12	119.3(3)	C50	C51	Ir2	118.4(2)
C16	C18	N19	109.7(2)	C50	C52	N53	109.3(2)
C18	N19	Ir1	108.27(17)	C52	N53	Ir2	107.59(16)
C20	N19	Ir1	116.05(17)	C54	N53	Ir2	115.24(17)
C20	N19	C18	110.7(2)	C54	N53	C52	110.4(2)
C20	N19	C36	109.5(2)	C54	N53	C70	109.3(2)
C36	N19	Ir1	102.00(17)	C70	N53	Ir2	108.80(17)
C36	N19	C18	109.9(2)	C70	N53	C52	105.0(2)
N19	C20	C21	115.2(2)	N53	C54	C55	114.6(2)
O22	C21	C20	109.8(2)	O56	C55	C54	110.1(2)
C21	O22	C23	113.1(2)	C55	O56	C57	112.8(2)
O22	C23	C24	112.3(3)	O56	C57	C58	112.3(3)
O25	C24	C23	108.7(3)	O59	C58	C57	108.6(3)
C24	O25	C26	112.4(2)	C60	O59	C58	112.0(3)
O25	C26	C27	107.6(3)	O59	C60	C61	108.4(3)

O28	C27	C26	109.1(3)	O62	C61	C60	109.0(3)
C29	O28	C27	113.0(3)	C61	O62	C63	111.5(3)
O28	C29	C30	109.0(3)	O62	C63	C64	109.3(3)
O31	C30	C29	110.5(3)	O65	C64	C63	110.0(3)
C30	O31	C32	110.9(3)	C64	O65	C66	111.8(3)
O31	C32	C33	109.4(3)	O65	C66	C67	108.9(3)
O34	C33	C32	108.4(3)	O68	C67	C66	107.6(3)
C33	O34	C35	113.3(2)	C67	O68	C69	113.6(2)
O34	C35	C36	115.5(2)	O68	C69	C70	108.6(2)
N19	C36	C35	118.2(3)	N53	C70	C69	116.2(2)

Table S13. Torsion Angles for (^{18c6}NCOP^{iPr})Ir(CO) (2^{18c6}).

A	B	C	D	Angle/°	A	B	C	D	Angle/°
Ir1	P2	C3	C4	-47.3(2)	Ir2	P3	C37	C38	-75.9(2)
Ir1	P2	C3	C5	75.9(2)	Ir2	P3	C37	C39	47.5(2)
Ir1	P2	C6	C7	54.1(2)	Ir2	P3	C40	C41	-172.92(17)
Ir1	P2	C6	C8	178.46(18)	Ir2	P3	C40	C42	-49.3(2)
Ir1	P2	O11	C12	-5.9(2)	Ir2	P3	O45	C46	13.8(2)
Ir1	N19	C20	C21	-55.0(3)	Ir2	N53	C54	C55	57.8(3)
Ir1	N19	C36	C35	175.3(2)	Ir2	N53	C70	C69	67.6(3)
P2	O11	C12	C13	-176.7(2)	P3	O45	C46	C47	170.7(2)
P2	O11	C12	C17	3.4(3)	P3	O45	C46	C51	-8.8(3)
C3	P2	C6	C7	-167.1(2)	C37	P3	C40	C41	47.5(3)
C3	P2	C6	C8	-42.7(3)	C37	P3	C40	C42	171.0(2)
C3	P2	O11	C12	-128.1(2)	C37	P3	O45	C46	138.1(2)
C6	P2	C3	C4	170.7(2)	C40	P3	C37	C38	65.3(2)
C6	P2	C3	C5	-66.1(2)	C40	P3	C37	C39	-171.3(2)
C6	P2	O11	C12	123.6(2)	C40	P3	O45	C46	-114.0(2)
O11	P2	C3	C4	68.1(2)	O45	P3	C37	C38	168.0(2)
O11	P2	C3	C5	-168.8(2)	O45	P3	C37	C39	-68.6(2)
O11	P2	C6	C7	-63.9(2)	O45	P3	C40	C41	-55.7(2)
O11	P2	C6	C8	60.4(2)	O45	P3	C40	C42	67.8(2)
O11	C12	C13	C14	179.9(3)	O45	C46	C47	C48	-179.7(3)
O11	C12	C17	Ir1	1.2(4)	O45	C46	C51	Ir2	-1.5(4)
O11	C12	C17	C16	179.6(3)	O45	C46	C51	C50	178.6(3)
C12	C13	C14	C15	0.7(5)	C46	C47	C48	C49	0.6(5)
C13	C12	C17	Ir1	-178.7(2)	C47	C46	C51	Ir2	179.0(2)
C13	C12	C17	C16	-0.3(5)	C47	C46	C51	C50	-0.9(5)
C13	C14	C15	C16	-0.7(5)	C47	C48	C49	C50	0.0(5)
C14	C15	C16	C17	0.2(5)	C48	C49	C50	C51	-1.1(4)

C14	C15	C16	C18	-176.4(3)	C48	C49	C50	C52	177.5(3)
C15	C16	C17	Ir1	178.7(2)	C49	C50	C51	Ir2	-178.3(2)
C15	C16	C17	C12	0.3(4)	C49	C50	C51	C46	1.5(4)
C15	C16	C18	N19	-157.6(3)	C49	C50	C52	N53	153.9(3)
C16	C18	N19	Ir1	-32.8(3)	C50	C52	N53	Ir2	36.7(2)
C16	C18	N19	C20	-161.1(2)	C50	C52	N53	C54	163.3(2)
C16	C18	N19	C36	77.8(3)	C50	C52	N53	C70	-79.0(3)
C17	C12	C13	C14	-0.2(5)	C51	C46	C47	C48	-0.2(5)
C17	C16	C18	N19	25.6(3)	C51	C50	C52	N53	-27.4(3)
C18	C16	C17	Ir1	-4.4(4)	C52	C50	C51	Ir2	2.9(3)
C18	C16	C17	C12	177.2(3)	C52	C50	C51	C46	-177.2(3)
C18	N19	C20	C21	68.9(3)	C52	N53	C54	C55	-64.3(3)
C18	N19	C36	C35	60.6(3)	C52	N53	C70	C69	-177.5(2)
N19	C20	C21	O22	-87.3(3)	N53	C54	C55	O56	91.4(3)
C20	N19	C36	C35	-61.2(3)	C54	N53	C70	C69	-59.0(3)
C20	C21	O22	C23	-164.3(2)	C54	C55	O56	C57	163.2(2)
C21	O22	C23	C24	93.2(3)	C55	O56	C57	C58	-91.4(3)
O22	C23	C24	O25	-66.1(3)	O56	C57	C58	O59	66.3(3)
C23	C24	O25	C26	177.3(2)	C57	C58	O59	C60	-176.4(2)
C24	O25	C26	C27	-165.0(3)	C58	O59	C60	C61	169.5(3)
O25	C26	C27	O28	71.6(3)	O59	C60	C61	O62	-71.9(4)
C26	C27	O28	C29	-177.4(3)	C60	C61	O62	C63	-175.1(3)
C27	O28	C29	C30	-176.5(3)	C61	O62	C63	C64	179.7(3)
O28	C29	C30	O31	-71.0(4)	O62	C63	C64	O65	77.8(4)
C29	C30	O31	C32	177.4(3)	C63	C64	O65	C66	179.5(3)
C30	O31	C32	C33	179.8(3)	C64	O65	C66	C67	175.9(3)
O31	C32	C33	O34	78.4(4)	O65	C66	C67	O68	-75.3(3)
C32	C33	O34	C35	179.6(3)	C66	C67	O68	C69	173.7(3)
C33	O34	C35	C36	77.8(3)	C67	O68	C69	C70	-177.3(2)
O34	C35	C36	N19	67.6(4)	O68	C69	C70	N53	83.8(3)
C36	N19	C20	C21	-169.8(2)	C70	N53	C54	C55	-179.3(2)